ISSN 0869-5938, Stratigraphy and Geological Correlation, 2017, Vol. 25, No. 1, pp. 39–75. © Pleiades Publishing, Ltd., 2017.
Original Russian Text © A.Yu. Guzhikov, E.Yu. Baraboshkin, V.N. Beniamovsky, V.S. Vishnevskaya, L.F. Kopaevich, E.M. Pervushov, A.A. Guzhikova, 2017, published in Stratigrafiya, Geologicheskaya Korrelyatsiya, 2017, Vol. 25, No. 1, pp. 24–61.

New Bio- and Magnetostratigraphic Data on Campanian–Maastrichtian Deposits of the Classical Nizhnyaya Bannovka Section (Volga River Right Bank, Southern Saratov Region)

A. Yu. Guzhikov[a], E. Yu. Baraboshkin[b], V. N. Beniamovsky[c], V. S. Vishnevskaya[c], L. F. Kopaevich[b], E. M. Pervushov[a], and A. A. Guzhikova[a]

[a]*Saratov State University, ul. Astrakhanskaya 83, Saratov, 410012 Russia*
[b]*Moscow State University, Moscow, 119991 Russia*
[c]*Geological Institute, Russian Academy of Sciences, Pyzhevskii per. 7, Moscow, 119017 Russia*
e-mail: aguzhikov@yandex.ru

Received December 25, 2015; in final form, January 20, 2016

Abstract—The integral investigation of the upper Campanian–Maastrichtian section near the settlement of Nizhnyaya Bannovka (Krasnoarmeiskii district, Saratov oblast) included its detailed lithological description and the study of different organic remains (belemnites, benthic and planktonic foraminifers, radiolarian, calcareous nannofossils, dinocysts) with the analysis of their taxonomic composition and stratigraphic distribution and magnetostratigraphic (magnetic polarity and petromagnetic) properties. The belemnite findings indicate the presence of the upper Campanian Belemnitella langei Zone in the section, which comprises sediments previously attributed to the lower Maastrichtian Belemnitella lanceolata Zone. The analogs of magnetic polarity chrons 33n, 32r, and 31n (probably superposed chrons 31n and 30) are established. It is assumed that radiolarians offer the opportunity to define the middle Campanian substage by analogy with the standard (international) stratigraphic scale. On the basis of benthic foraminifers, calcareous dinocysts, and paleomagnetic data, the late Maastrichtian age of sediments previously dated back to the early Maastrichtian is substantiated. A large hiatus corresponding to the terminal Campanian–early Maastrichtian is revealed in the section. The succession of sedimentological, biotic, and paleogeographic events is outlined for the late Campanian–Maastrichtian interval. The obtained data make it possible to disclose paleobiogeographic connections between microfaunal communities of the Campanian and late Maastrichtian seas on the East European and West Siberian plates. It is established that the uppermost Maastrichtian sediments are enriched in extraterrestrial matter.

Keywords: Campanian, Maastrichtian, belemnites, radiolarians, benthic and planktonic foraminifers, calcareous nannofossils and dinocysts, magnetostratigraphy, biostratigraphy, paleobiogeography, East European Platform, Volga region

DOI: 10.1134/S0869593817010026

INTRODUCTION

In 2001, the Interdepartmental Stratigraphic Committee (ISC) of Russia considered and approved the Upper Cretaceous stratigraphic scale for the East European Platform (EEP) within limits of the Russian Federation (Olfer'ev and Alekseev, 2003, 2005; *Stratigraficheskaya*..., 2004) widely used now in stratigraphic investigations. During the subsequent 14 years, the investigations initiated by A.G. Olfer'ev to perfect this scale through the integral study of Upper Cretaceous sections of the southern East European Platform in Saratov (Olfer'ev et al., 2004, 2007, 2008, 2009a, 2009b, 2014; Guzhikova and Bagaeva, 2013; Guzhikov et al., 2014b; Pervushov et al., 2015), Volgograd (Aleksandrova et al., 2012), and Rostov (Beniamosky et al., 2012, 2014) oblasts and in the Aktolagai Plateau area in Aktyubinsk oblast of Kazakhstan (Guzhikov et al., 2014a) were in progress. These investigations yielded new sedimentological, paleontological, and, recently (2013–2015), magnetostratigaphic and isotopic data.

The Nizhnyaya Bannovka section is located on the right bank of the Volga River, 1.5–2 km to the south from the Nizhnyaya Bannovka settlement of the Krasnoarmeisk district, south Saratov region. It is studied in two outcrops located ~1 km from each other: outcrop 3012 at the head of the Mozhzhevelovyi Ravine (coordinates 50°42′57.4″ N, 45°38′26.7″ E) and outcrop 3011 located on the southern slope of Mount Syrt

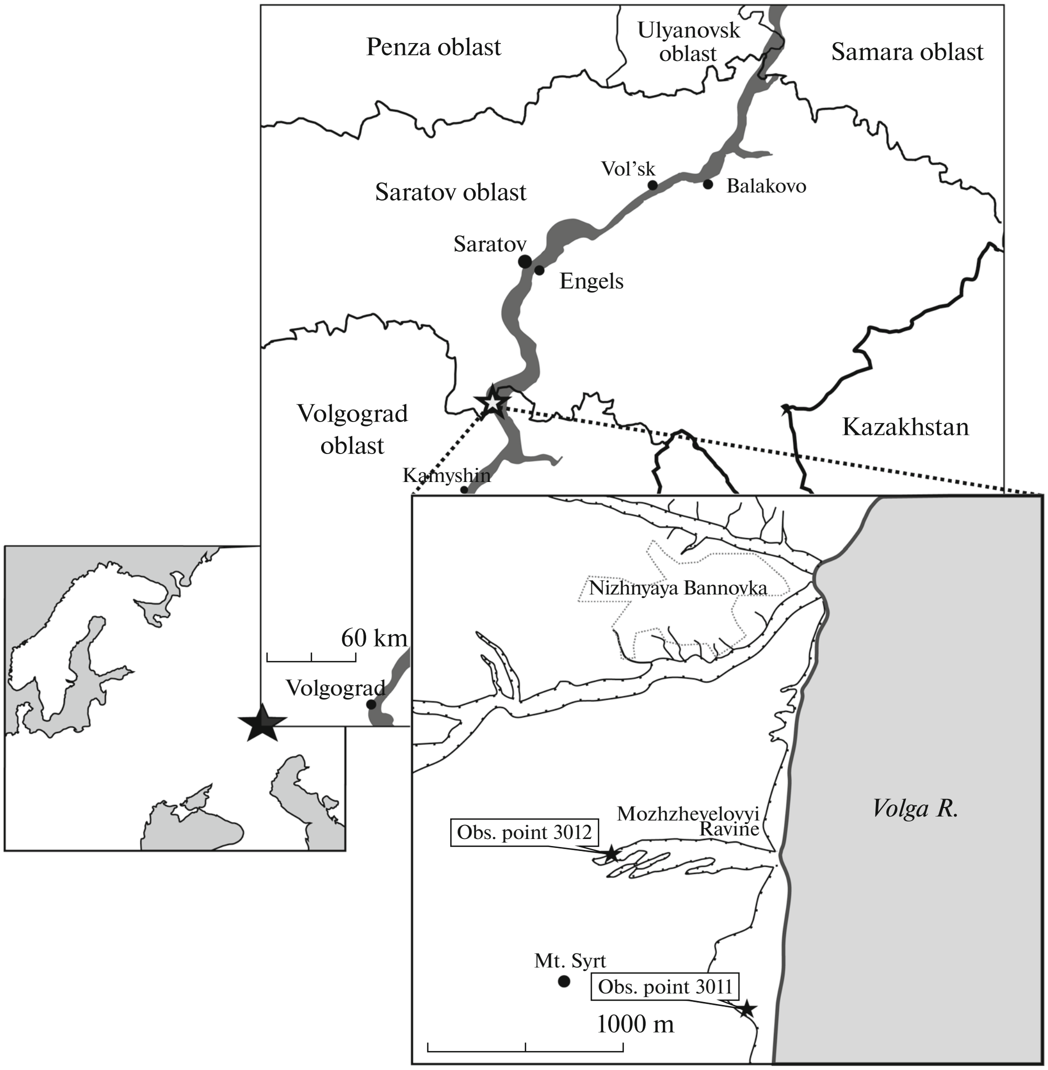

Fig. 1. Schematic location of Campanian–Maastrichtian outcrop near the settlement of Nizhnyaya Bannovka (designated by asterisks).

facing the Volga River (coordinates 50°42′29.8″ N, 45°38′59.4″ E) near the landslide scarp (Figs. 1, 2).

The Nizhnyaya Bannovka section was visited in 2012 and 2014 for its additional study and sampling for different analyses. The samples for simultaneous micropaleontological, paleomagnetic, and petromagnetic analyses were taken in parallel with geological description of the section from 106 levels of the 60-m-thick section (Fig. 3). The fundamentally new approach used in these works consisted in the application of the magnetostratigraphic method together with others for the study of Upper Cretaceous reference sections of the East European Platform.

The investigations included lithological description of the section (E.M. Pervushov and A.Yu. Guzhikov), paleo- and petromagnetic measurements (A.A. Guzhikova), and study of different macro- and microfossils: belemnites (E.Yu. Baraboshkin), sponges (E.M. Pervushov), radiolarians and calcareous dinocysts (V.S. Vishnevskaya), benthic foraminifers (V.N. Beniamovsky), planktonic foraminifers (L.F. Kopaevich), calcareous nannofossils (M.N. Ovechkina and M.A. Ustinova). The efforts to extract palynomorphs from examined samples undertaken by N.K. Lebedeva (Institute of Petroleum Geology and Geophysics, Siberian Branch, Russian Academy of Sciences, Novosibirsk) appeared to be a failure.

BRIEF REVIEW OF THE SECTION STUDY

The expressive outcrops of Upper Cretaceous rocks on the right bank of the Volga River in the southern part of the Saratov region attracted the attention of geologists at the end of the 19th century, when local fishermen reported to the Archive Commission of the Saratov Province on findings of fossilized organic

(a)

(b)

Fig. 2. Photographs of outcrops 3012, Mozhzhevelovyi Ravine (a), and 3011, Mount Syrt (b). Lines and numerals designate boundaries of members and their numbers.

remains in the outskirts of settlement of Nizhyaya Bannovka. After investigations of sections on slopes of Mount Syrt and in the Mozhzhevelovyi Ravine south of this settlement carried out by outstanding Russian geologists (Arkhangelsky, 1912; Arkhangelsky and Dobrov, 1913; Milanovskii, 1940), they were considered as reference sections of Cretaceous deposits for the Middle and Lower Volga regions. During the field excursion organised in the framework of the All-Russian Conference on Specification of the Unified Mesozoic Stratigraphic Scale for the East European Platform, precisely these sections were visited (*Resheniya*..., 1955, 1962). In the second half of the 20th century, several researchers (Baryshnikova et al., 1961; Bondareva et al., 1981; Bondarenko, 1990; etc.) visited this section again to describe repeatedly its structure and lithology and gain additional paleontological material (including macrofossils) for subdivision of the section

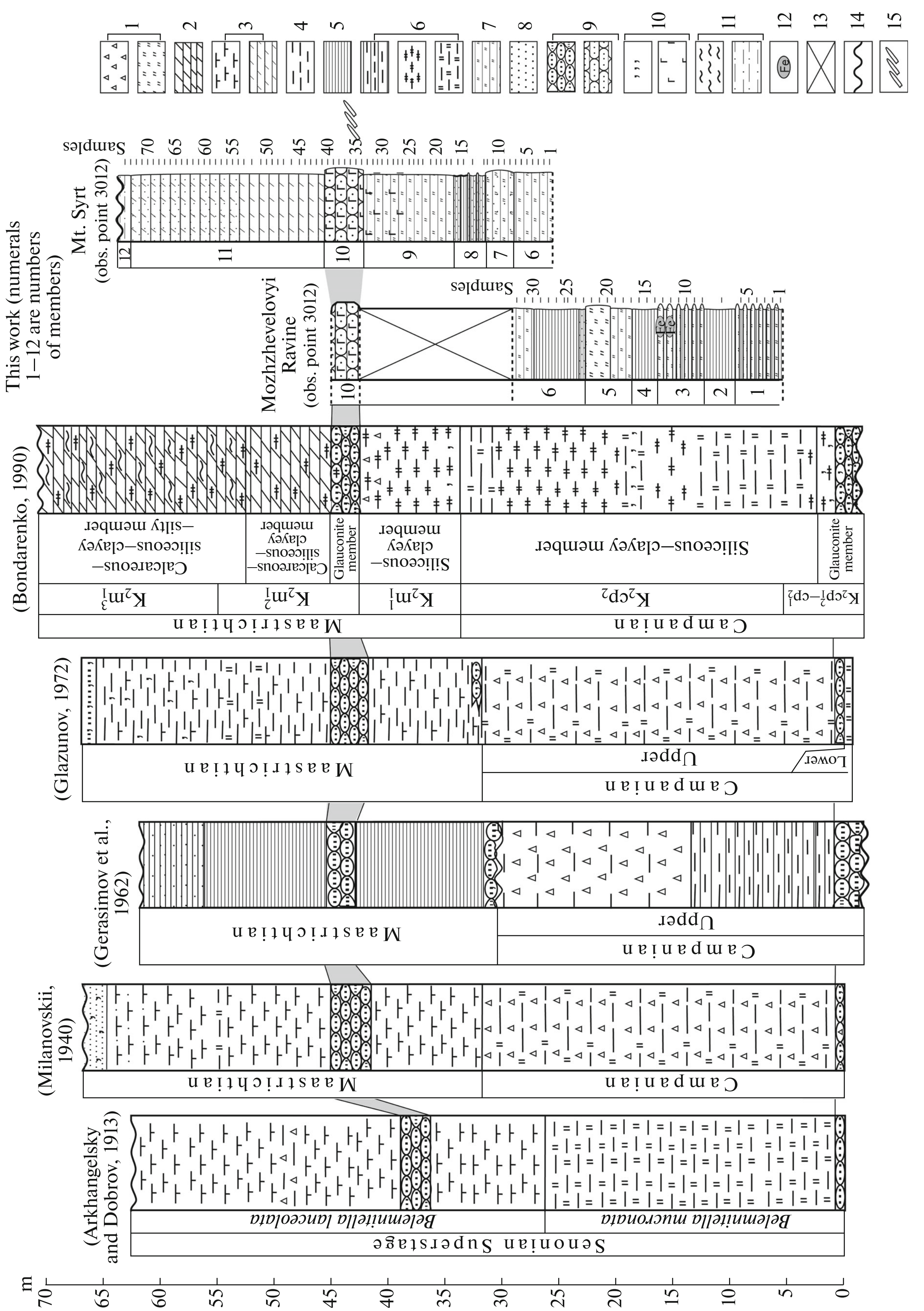

Fig. 3. Comparison of views of different researchers on the structure of the upper Campanian– upper Maastrichtian section of Mount Syrt (original lithological symbols are preserved). (1) Opokas; (2) marlstones; (3) carbonate cays; (4) clayey material; (5) clays (in this work, siliceous clays; in Gerasimov et al., 1962, likely carbonate clays); (6) siliceous clays; (7) opoka-like clays; (8) sandy material; (9) sandstone; (10) glauconite; (11) fine-grained sandy and silty material; (12) intense ferrugination; (13) unexposed; (14) hiatus; (15) belemnite finds.

into substages and zones. The current views on stratigraphy of the Campanian–Maastrichtian boundary interval are summarized in (Pervushov et al., 1999b). According to those authors, the composite section in the head part of the Mozhzhevelovyi Ravine and on Mount Syrt slopes includes the upper Campanian substage uniting the belemnite langei and licharewi zones (siliceous–terrigenous sequence) and lower Maastrichtian substage represented by the lanceolata Zone (terrigenous–carbonate sequence).

The attempts to apply the paleomagnetic method to the study of the Upper Cretaceous section in the Nizhnyaya Bannovka area undertaken in the 1980s (Pechersky et al., 1983; Grishanov, 1984; Abakshin et al., 1992) appeared to be a failure because of extremely low natural remanent magnetization of rocks undetectable by the measuring equipment of that time. At the same time, petromagnetic data on the section were necessary for obtaining new information about depositional environments (Fomin et al, 2006)

SECTION STRUCTURE

In the section, all of its layers are subhorizontal. With respect to lithology, it is distinctly divisible into two parts: lower siliceous–terrigenous (Members 1–9) and upper terrigenous–carbonate (Members 10–12) sequences traditionally correlated with the Altyn Superformation and Lokh Formation, respectively (*Stratigraficheskaya*..., 2004).

Below, the composite section is described from the base upward (Fig. 3).

Outcrop 3012 (Mozhzhevelovyi Ravine)

Member 1 (Samples 3012/1–3012/6). Frequently alternating dark gray (locally with the bluish tint) to light gray opokas (from 10 to 30 cm thick) and dark gray to black platy to foliated clays (usually up to 0.1 m thick). Both opokas and clays are locally micaceous and contain frequently irregularly distributed psammitic fine- to medium-grained quartz and glauconite material in concentrations highly variable in different layers. The psammitic material is largely confined to abundant differently oriented burrows 0.1–1.0 cm in diameter and 0.5–5.0 cm long. All rocks are irregularly fractured and ferruginate to different degrees on the surface and along fractures. The upper layers of the member form a steep scarp in erosional ridges. The apparent thickness is ~4 m.

Member 2 (Sample 3012/7). Black clays, siliceous, foliated. The upper part of the member includes two intercalations of finely splintered opoka 0.2–0.3 m thick. The thickness is 2.5 m.

Member 3 (Samples 3012/8–3012/13). Frequently alternating opokas and siliceous clays similar to these varieties in Member 1. The peculiar feature of its upper half is the presence of closely spaced thick (0.4–0.5 m) opoka layers highly ferruginate at the surface. The uppermost part of Member 3 also forms a steep scarp in erosional ridges. The thickness is 4.2 m.

Member 4 (Samples 3012/14–3012/16). Dark gray to black opoka-like clays, siliceous, finely splintered. The boundary with the overlying member is indistinct. The thickness is 2.5 m.

Member 5 (Samples 3012/17–3012/22). Opokas and gray opoka-like clays without distinct boundaries between them. In the upper part of the member, the surface of opoka layers acquires a peculiar greenish tint. The thickness is 4 m.

Member 6 (Samples 3012/23–3012/32). Dark gray to black clays, siliceous, sandy, finely splintered, foliated. In the basal pat of the member, clay is gray, highly sandy, ~0.3 m thick; in the upper part (Samples 3012/30–3012/32), clays are opoka-like. The apparent thickness is 6.5 m.

The overlying sediments are poorly exposed. At the same time, many gullies crossing the northeastern slope of Mount Syrt 13–15 m higher in the section recover everywhere glauconite sandstone saturated with belemnite rostra and oyster shells (Member 10), which served as a reference level for correlation between outcrops 3012 and 3011. A more reliable correlation was provided by paleo- and petromagnetic data.

Outcrop 3011 (Mount Syrt)

In the outcrop on the southern slope of Mount Syrt, the upper part of Member 6 (the apparent thickness of ~3.5 m) was repeatedly sampled (Samples 3011/1–3011/7). The contact with the overlying member is obscure. The integral thickness of Member 6 in two outcrops is 7–9 m.

Member 7 (Samples 3011/8–3011/12). Dark gray opokas, clayey, sandy, with thin intercalations of siliceous sandy clays. At the surface, Members 6 and 7 are covered by rubble of light gray opoka-like rocks with the boundary between them being unobservable. The thickness is 2.4 m.

Member 8 (Samples 3011/13–3011/16). Dark gray to dark brown (most likely owing to iron hydroxides) clays, siliceous, highly sandy, finely splintered, with subordinate intercalations of opoka-like clays. The entire surface of the member is covered by gray–brown rubble. The thickness is 2.8 m.

Member 9 (Samples 3011/17–3011/33). Dark gray clays, opoka-like, sandy, micaceous. Approximately 5 m above the base, the member contains visible glauconite grains, abundance of which notably increases upward. The content of the silty and fine-grained quartz material dispersed or forming lenses increases in the same direction. Burrows are rare and chaotically distributed, being expressed as spots at the weathered surface. Combination of relict thin lamination and burrows imparts a variegated appearance to the host rock. The surface of the member is covered by greenish rubble. The thickness is 8 m.

Members 8 and 9 form a peculiar gentle slope between two benches formed by over- and underlying rocks in the microrelief of the Mount Syrt slope.

Member 10 (Samples 3011/34–3011/40). Yellow-green sandstone, glauconite–quartzose, carbonate, fine- to medium-grained, vaguely bedded; bright green at the fresh surface, spotty owing to irregular distribution of light gray iron hydroxides. The distribution of the terrigenous and carbonate components is also irregular. Upward, the content of the psammitic component and its grain size decrease, while the carbonate content increases, which is evident from the reaction with HCl: its absence in the basal part of the member (up to the level of Sample 3011/37) to strong ebullience in the uppermost part. Brown phosphorite nodules up to 3–4 cm across are also irregularly scattered through the rock. Phosphorites are fusiform, representing fossilized and reworked casts or walls of burrows. Bioturbation is represented by small thin hollows.

The lower boundary of the member is obscure. Sandstones from the basal part of the member resemble opoka-like sand-rich clays with a high content of glauconite constituting the uppermost part of Member 9. The upper boundary of the member is distinct and uneven. At the top, sandstone is poorly consolidated, with thin parallel lamination, which is emphasized by the thin platy jointing; burrows in the upper part of the member are larger and longer than in its remainder.

The lower part of the member is saturated with vertebrate remains. Molluscan shells dominated by oysters are also scattered in abundance. They are represented by *Pycnodonte concavexa* (Sow.), *P. variabile* A. Ivanov, *Auriphyllina mirabilis* (Rousseon), *Volgella porrecta* A. Ivanov, *V. oblique* A. Ivanov, *V. sculpta* A. Ivanov, *Orbigonia* cf. *civaliaris* A. Ivanov, *Vanustella subdonetzensis* (Glassunova), *Vanustella* sp., and *Hyotissa* sp. accompanied by isolated thin valves of *Chlamys* sp. *Ostrea* shells are large (up to 8–10 cm across); they are frequently represented by whole shells. There are also abundant belemnite rostra oriented usually by their apical parts in the horizontal plane in different directions; some of them located diagonally, being oriented by their apexes downward. Many rostra are longitudinally compressed in the dorsal–ventral direction almost up to the flat state. The rocks contain also rare accumulations and isolated small dark brown fish scales. Close to the base, the sediments enclose skeletons of hexactinellid sponges *Ortodiscus* sp. and *Rhizopoterion* sp. buried in the subautochthonous position. As in the largest part of the Volga River right bank area, the lower part of the member contains variably phosphatized marine reptilian remains.

The outcrops of irregularly consolidated sandstone form a small bench in the relief profile of Mount Syrt. The thickness of the member is 3.5 m.

Member 11 (Samples 3011/41–3011/72). Light to dark gray clays, carbonate, silty–sandy, marlstone-like in the lower part of the member and highly silty–sandy in its upper part. The conditional boundary between these varieties is outlined at the sustained level of subvertical burrows irregularly colored by iron hydroxides (Sample 3011/5 level). The sediments contain dispersed small mica flakes and fine-grained glauconite, abundance of which increases upward similarly to quartz psammitic particles. There are also thin (<1 cm) intercalations of clays, yellow-colored owing to the presence of iron hydroxides. The thickness is 17 m.

Member 12 (Samples 3011/73, 3011/74). Silt, clayey, carbonate-free, yellow-colored owing to iron hydroxides, with glauconite grains and small bivalve shells and single belemnite rostra (Pervushov et al., 1999a) scattered at some levels, irregularly bioturbated. The upper surface of the member is distinct, uneven, locally with pockets. The thickness is up to 1 m.

Higher in the section, these strata are overlain by siliciliths of the Paleocene Syzran Formation.

We compared different views on the structure of the Nizhnyaya Bannovka section (Mozhzhevelovyi Ravine, Mount Syrt). In doing so, we took two beds of glauconite sandstones as readily recognizable reference levels: lower (Campanian) with *Belemnitella mucronata* (Bed 8 according to (Milanovskii, 1940)) and upper (Maastrichtian) with *B. lanceolata* (Bed 3 after Milanovskii (1940) or Member 10 in this work)) (Fig. 3). The data on the thickness of sediments sandwiched between these beds are satisfactorily consistent between each other in different publications. The interval in question includes thin glauconite intercalations, which are missing in some descriptions, being characterized by a lenticular structure. The discordance consists also in the presence/absence of the member of carbonate clays below the upper bed of glauconite sandstones, which is mentioned in some descriptions (Arkhangelsky and Dobrov, 1913; Milanovskii, 1940; Gerasimov et al., 1962; Glazunova, 1972) and is absent in others (Bondarenko, 1990; this work). Arkhangelsky and Dobrov (1913) were the first to define a member of "gray calcareous clays" 10–15 m thick on Mount Syrt. We failed to document carbonate sediments below the base of sandstone Member 10 in the continuous succession on the southern bedrock slope of Mount Syrt undistorted by landslides; instead, we observed alternating siliceous clays and opokas (Members 6–9), which is consistent with the thorough description of the section in (Bondarenko, 1990) Fig. 3). The surface of this sequence is covered by eluvial rubble. According to our observations, Members 7–12 are now unexposed in the Mozhzhevelovyi Ravine head (northern slope of Mount Syrt). At the same time, the upper glauconite sandstone (Member 1) may be observable and traceable in shallow scours and rubble accumulations. The underlying siliceous rocks (Members 7–9) 13–15 m thick are unexposed, being covered by vegetation, carbonate eluvium, and talus, which may easily be taken off the weathered surface of the carbonate clay bedrock. Milanovskii (1940) noted poorly exposed sediments in this portion of the section. In this connection, we believe that the carbonate member 10–15 m thick underlying glauconite sandstone was defined by some authors erroneously. It is conceivable that the effect of the first description of "gray calcareous clays" was partly responsible for this error. For example, Glazunova (1972) openly indicates that she used the description in (Milanovskii, 1940) when compiling her lithological column.

BIOSTRATIGRAPHY

Materials and Methods

The subdivision of the section under consideration is based on findings and biostratigraphic analysis of different macro- and microfossils: belemnites, benthic and planktonic foraminifers, radiolarians, nannofossils, and calcareous dinocysts.

In total, 106 samples each weighting at least 200 g were taken for paleontological investigations (together with oriented samples for paleomagnetic measurements) every 0.2–0.4 m (Fig. 3). All the belemnite finds originate from Member 10.

Foraminifers were extracted from samples (100 g in weight) washed in accordance with the standard technique in the laboratory of the Chair of Paleontology (Faculty of Geology, Moscow State University). Only three samples from the terrigenous–siliceous sequence (Members 1–9) contained single planktonic foraminiferal specimens. Carbonate clays of Member 11 (12 samples) yielded relatively diverse and abundant foraminifers. None of their tests was found in sediments of Members 10 and 12.

Radiolarians occur in the same samples more frequently (in 21 samples from siliceous rocks). They are also present in nine samples from the lower part of the carbonate clay sequence. Radiolarians were studied in both residues and thin sections.

Foraminifers, radiolarians, nannofossils, and calcareous dinocysts were photographed under the scanning microscope at the Paleontological Institute of the Russian Academy of Sciences. Belemnites preliminarily covered with ammonium chloride were photographed by a SONYα580 camera with a SONY Macro 2.8/50 objective.

The illustrated specimens are stored in two laboratories of the Geological Institute of the Russian Academy of Sciences: laboratory of micropaleontology (collection NB 3011–3012: foraminifers) and laboratory of biostratigraphy and paleogeography of oceans (collection NB 3011–3012: radiolarians, calcareous dinocycts, and nannofossils). The collection of belemnites is stored in the Earth Science Museum of Moscow State University (collection no. 126).

Belemnites

First data on belemnite finds in the Campanian–Maastrichtian interval of the Nizhnyaya Bannovka section are mentioned in (Sinzow, 1899). This researcher indicated "*Belemnitella lanceolata* (Schloth.) Sharpe" (Sinzow, 1899, p. 69) for the marlstone sequence near the settlements of Zolotoe, Trubnoe, Bannoe, and Melovoe, figured it under the name "*Belemnitella sublanceolata* Sharp." (Sinzow, 1899, plate IV, figs. 3–4). Subsequently, Arkhangelsky (1912) identified this form as *Actinocamax propinquus* Moberg. He studied the section under consideration as well and defined the "Belemnitella lanceolata Schlth. (Sn. s. 2)" Zone, including in it the sequence of gray clays grading into clayey marlstones and clayey glauconite sands and sandstones. The middle part of this sequence contains abundant species indicated in (Milanovskii, 1940; Glazunova, 1972). The data on Campanian–Maastrichtian deposits in the Nizhnyaya Bannovka section and presence of the Belemnitella licharewi, B. lanceolata, and B. sumensis zones in them are also available in (Arkhangelsky and Dobrov, 1913; Gerasimov et al., 1962; Bondarenko, 1978; Grishanov, 1984; Pervushov et al., 1999a, 1999b; Gabdullin, 2002; Yakovishina et al., 2012), although none of these authors provided identifications of belemnites and their stratigraphic distribution. It is strange, but no single image of belemnites from this locality, except for the above-mentioned "*Belemnitella sublanceolata* Sharp.," may be found in corresponding publications. It is probable that this circumstance explains why our results differ from traditional data.

In the section, belemnites were found only in glauconite sandstones of Member 10 (single rostra were also noted in the Member 12, but their taxonomic affinity remains unknown (Pervushov et al., 1999a)). Most findings without indications of substantial reworking originate from the lower part of the member (below Sample 3011/38). Belemnite rostra at levels of Samples 3011/38 and 3011/39 are partly dissolved and deformed. Of 22 rostra, 17 specimens appeared to be identifiable. They are largely represented by *Belemnitella pseudolanceolata* Jeletzky, 1948 (accompanied by *B.* cf. *pseudolanceolata* and *B. pseudolanceolata* juv. (Plate I)), except for a single specimen of *Belemnitella langei* Jeletzky, 1948 (Plate I). Both forms are established in this locality for the first time instead of *Belemnitella lanceolata* (Schloth.), which was traditionally reported from here. This fact is surprising. Nevertheless, despite the distinct lanceolate shape and large size of rostra, which lead to error, *Belemnitella pseudolanceolata* is characterized by high values of the Shatsky index (distance from the alveolar apex to the inner end of the ventral fissure) varying from 6.0 to

Plate I. Belemnites from the Nizhnyaya Bannovka section (Member 10). (1a–1d) *Belemnitella pseudolanceolata* juv. Jeletzky, 1948, specimen MES MSU 126/1; (2a–2d) *Belemnitella langei* Jeletzky, 1948, specimen MES MSU 126/2; (3a–3d) *Belemnitella pseudolanceolata* Jeletzky, 1948, specimen MES MSU 126/3; (4a–4d) *Belemnitella pseudolanceolata* Jeletzky, 1948, specimen MES MSU 126/4. Collection of belemnites is stored in the Museum of Earth Sciences (Moscow State University), no. 126. For all specimens: (a) dorsal view, (b) ventral view, (c) lateral view, (d) structure of the ventral fissure. All specimens originate from Member 10, interval of Samples 34–37, Section 3011; Mount Syrt near settlement of Nizhnyaya Bannovka. Samples are covered with ammonium chloride and photographed by E.Yu. Baraboshkin using a SONYα580 camera equipped with a SONY Macro 2.8/50 objective. Scale bar is 1 cm.

16.2 mm, which is characteristic of representatives of the genus *Belemnitella*.

Among known belemnite species described from Campanian–Maastrichtian sections of the East European Platform and Western Europe, only *B. kursensis* (Najdin, 1964) and *B. pseudolanceolata* Jeletzky, 1948 are characterized by close sizes, shapes, and Shatsky index values. Jeletzky (1949) attributed the latter species to the genus *Belemnitella*. Naidin (1959) also considered this species as belonging to the same genus, although he subsequently placed *B. pseudolanceolata* into the genus *Belemnella*, proceeding from the morphology of rostra.

European specialists always considered these two species as representatives of the genus *Belemnitella*. Since *B. kursensis* is missing in European sections, only *B. pseudolanceolata* was discussed. Christensen (1986, p. 37) believed that this form is close to *Belemnitella langei*, although later (Robaszynski and Christensen, 1989; Christensen, 1990), he conceded, similarly to Jeletzky (1948), its synonymy with *Belemnites lundgreni* de Morgan, 1882. Inasmuch as the last assumption is impossible to verify because of inaccessibility of type material, Christensen admitted, following Schulz (1979), the autonomous status of *B. pseudolanceolata*, but attributed it to the genus *Belemnitella* on the basis of large values of the Shatsky index (Christensen, 1993). Subsequently, Christensen (1995) placed it into the *Belemnitella mucronata* group. It is remarkable that no illustrations or valuable descriptions of *B. pseudolanceolata* Jeletzky appeared in publications after the work by (Jeletzky, 1948). All this indicates that either the species in question is missing from West European sections (which is quite possible taking into consideration high endemism of Late Cretaceous belemnites) or it was ignored in connection with the above-mentioned problems.

According to (Naidin, 1959, 1961; Gerasimov et al., 1962), *B. pseudolanceolata* is characteristic of the langei Zone, which is confirmed in our case by a single finding of *B. langei* Jeletzky (Plate I, figs. 1a–1d). This form slightly differs from typical representatives of *Belemnitella langei langei* in relatively small size, Shatsky index value (4.2 mm), and distinctly fusiform shape. It is slightly closer to *Belemnitella langei najdini* Kongiel, 1962 (according to Naidin), although attribution of a single specimen to this subspecies is premature.

As was shown (Christensen, 1999), there is no uniform view on the species *B. langei* and its stratigraphic position among Jeletzky, Birklund, Kongiel, Schulz, Naidin, and Christensen himself. Therefore, taking this ambiguity and scarcity of factual material into consideration, it is more logical, in our opinion, to follow the concept by Naidin.

Thus, identified belemnite specimens indicate the belonging of glauconite sandstones of Member 10 to the upper Campanian Belemnitella langei Zone.

Planktonic Foraminifers

Single tests of planktonic foraminifers (PF) are registered in the basal part of Member 11 (Samples 3011/44–3011/47). They are represented by *Heterohelix striata* (Ehrenb.) of the family Heterohelicidae (Plate II), which allows the Heterohelix striata Beds to be defined (Fig. 4). This species is very close to *H. planata* (Cushman), which is distributed through the Gan'kino Formation (uppermost Campanian–Maastrichtian) of West Siberia, although being most abundant and represented by typical specimens in its upper Maastrichtian interval (Marinov et al., 2014, pl. II, figs. 5–6**)**. *Heterohelix striata* is accompanied by single poorly preserved specimens of Globigerinelloides *volutus* White. Unfortunately, the assemblage of planktonic foraminifers in the Nizhnyaya Bannovka section is substantially scarcer as compared with other examined sections of the Middle Volga (Saratov) region.

For example, representatives of heterohelicids (particularly, genus *Heterohelix*) are abundant in upper Maastrichtian sections of the Teplovo uplift located approximately 65 km northeast of Saratov. In this area, Heterohelicidae representatives at some levels in the upper Maastrichtian Nikolaevskoe Formation of the section located near the settlement of Klyuchi exceed 80% of the foraminiferal paleocoenosis (Alekseev et al., 1999). They are accompanied by relatively diverse keeled *Globotrucana* forms, which reflect transgression of a late Maastrichtian warm epicontinental sea (Alekseev et al., 1999; Ovechkina and Alekseev, 2004; Kopaevich, 2011).

Benthic Foraminifers

The siliceous–terrigenous rocks of Members 1–9 contain single tests of "primitive" agglutinated foraminiferal species: *Haplophragmoides* sp. and *Rhabdammina* sp. in Member 3 (Sample 3012/9), *Ammodiscus* aff. *incertus* d'Orb. and *A. cretaceous* (Reuss) at the

Plate I

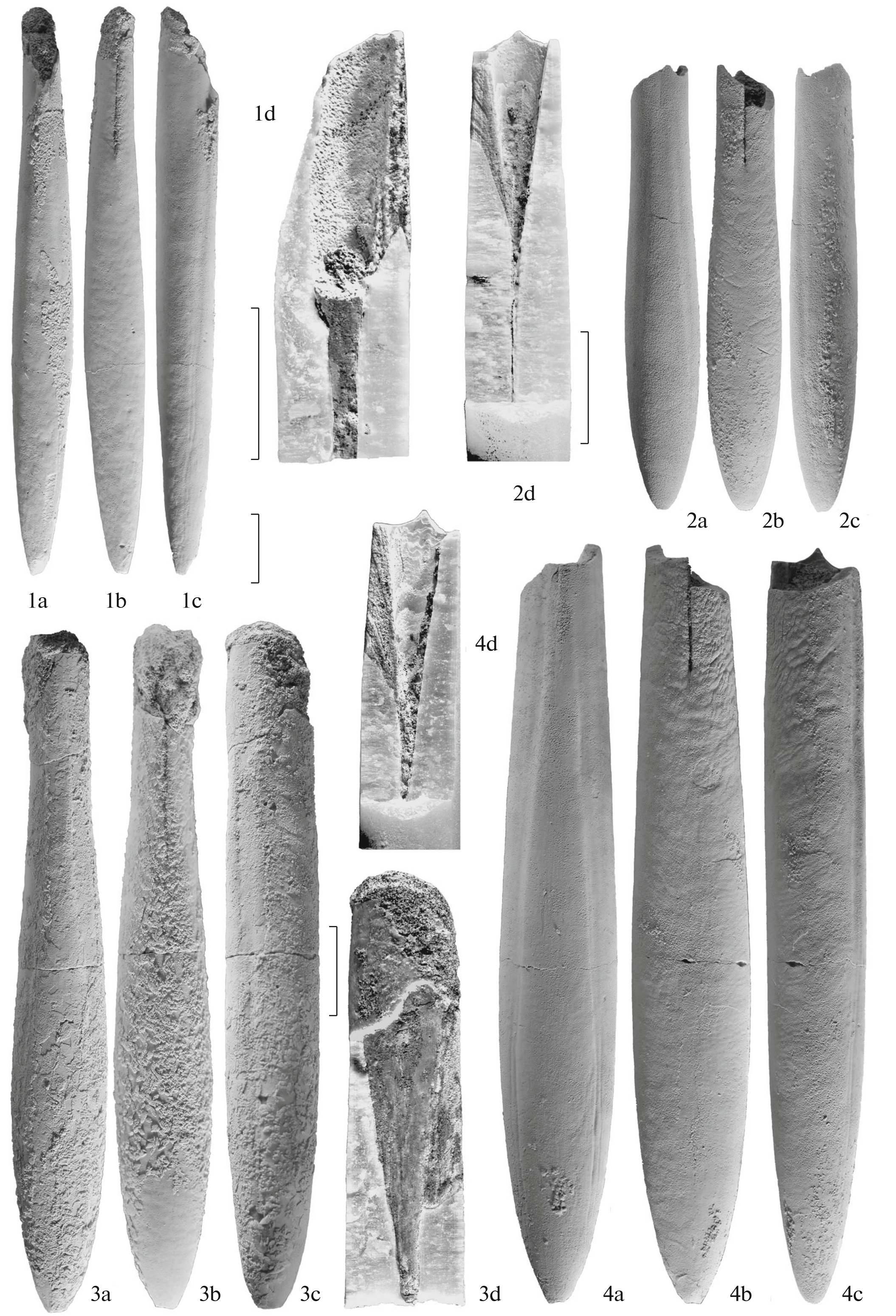

Plate II. Benthic foraminifers (Members 1–9), planktonic forminifers, and calcareous dinocysts (Member 11) from the Nizhnyaya Bannovka section. (1–13) Benthic foraminifers from Members 1–9: (1) *Rhabdammina* sp., general view, Sample 3012-9; (2) *Reophax* sp., general view, Sample 3011-27; (3, 4) *Psammosphaera* sp., general view, Sample 3011-27; (5) *Ammodiscus cretaceous* (Reuss), general view, Sample 3012-23; (6) *A.* aff. *incertus* d'Orb., general view, Sample 3012-23; (7, 8) *Haplophragmoides* sp., general view, Samples 3012-9 and 3011-27, respectively; (9–11) *Trochammina* sp., Sample 3012-23 (fig. 9) and Sample 3011-27 (figs. 10 and 11); (12, 13) *Silicosigmoilina volganica* (Kuzn.), general view (fig. 12), apertural view (fig. 13), Sample 3011-27; (14, 15) planktonic foraminifers from Member 11: *Heterohelix striata* (Ehrenb.), general view, Sample 3011-44; (16) calcareous dinocysts from Member 11: *Pithonella globosa*, Futterer, Sample 3011-44: (a) general view, (b) structure of the outer layer with wall of the *Pithonella* type, (c) fragment of the structure of trigonal calcite crystals.

base of Member 6 (Sample 3012/23), and ***Silicosigmoilina volganica*** **(Kuzn.),** *Psammosphaera* sp., *Reophax* sp., *Haplophragmoides* sp., and *Trochammina* sp. in Member 9 (Sample 3011/27) (Fig. 4, Plate II).[1] *S. volganica* is the characteristic form of foraminiferal assemblages from the Nalitovo Formation (uppermost Campanian) in the section near the settlement of Vishnevoe located north of Saratov (Olfer'ev et al., 2007) and from the Sukhodol Formation (Campanian–Maastrichtian boundary interval) in the Kalitva River sections in northern Rostov oblast (Beniamovsky et al., 2012). Thus, the presence of *S. volganica* provides grounds for attributing host sediments to the LC19 Zone, which encloses the Campanian–Maastrichtian boundary on the East European Platform (Guzhikov et al., 2014a, 2014b).

The diverse assemblage of benthic foraminifers (BF) appears beginning from the basal part of Member 11. The analysis of their distribution through the section allows two assemblages to be defined (Fig. 4, Plate III). They are named after most frequent species of paleobiogeographic and stratigraphic significance.

The lower assemblage (Spiroplectammina kasanzevi Beds) is present in the interval from Sample 3011/42 to Sample 3011/58 and includes ***Spiroplectammina kasanzevi*** **Dain**, *S. variabilis* (Neckaja), *Nodosaria* sp., *N. raphanistrum* (Linne), *Robulus* sp., *R. roemeri* (Reuss), *R.* velascoensis (Marie), *Lenticulina* sp., *L. exorata* (Hagen.), *L. osnabrugensis* Roemer, *Dentalina* sp., *D. filiformis* Reuss, *Vaginulinopsis* sp., *V. trilobatus* (d'Orb.), *Vaginulina* sp., *Astacolus* sp., *Planulina* sp., *Neoflabellina reticulata* (Reuss), *Globulina lacrima* Reuss, *G. veronikae* (Dain), *Pyrulina fusiformis* (Roemer), *Guttulina trigonula* (Reuss), *G. cretacea* Alth, *Gyroidinoides globosa* (Hagen.), *G. turgidus* (Hagen.), *Valvulineria formosa* Freim., *Pullenia* aff. *bulloides* (d'Orb.), *Gyromorphina allomorphinoides* (Reuss), *Nodogenerina* sp., *N. pseudoscripta* (Cushm.), and *Bulimina quadrata* Plummer. The S. kasanzevi Zone is established in the upper Maastrichtian Gan'kino regional stage of West Siberia (*Foraminifery*..., 1964).

The upper assemblage (Anomalinoides pinguis Beds) appears at the level of Sample 3011/58. As compared with the lower assemblage, its composition differs on account of appearance of characteristic species ***Anomalinoides pinguis*** **(Jennings)**, *A. globigeriniformis* (Neckaja), *Cibicidoides bembix kasahstanicus* (Neckaja), and *Cibicides beaumontianus* (d'Orb.). The Anomalinoides pinguis Zone characterizes the upper Maastrichtian interval of Poland (Gawor-Beidova, 1992). The Anomalinoides pinguis Beds were also established in the uppermost Maastrichtian sediments of the Aktolagai Plateau area, where they contain also upper Maastrichtian representatives of the genus *Neobelemnella* (*N. kazimiroviensis*) (Naidin and Beniamovsky, 2006).

A peculiar feature of the benthic foraminiferal assemblage from Member 11 is its significant similarity (up to 80%) to that from Maastrichtian carbonate clays of the Gan'kino Formation of West Siberia. The following species are in common for these assemblages: *Spiroplectammina variabilis*, *Nodosaria raphanistrum*, *N. glorja, Robulus roemeri*, *Dentalina filiformis*, *Globulina lacrima*, *G. veronikae*, *Pyrulina fusiformis*, *Guttulina trigonula*, *G. cretacea*, *Gyroidinoides soldanii*, *G. turgidus*, *Valvulineria formosa*, *Pullenia* aff. *bulloides*, *Gyromorphina allomorphinoides*, *Bulimina quadrata*, *Anomalinoides pinguis*, *A. globigeriniformis*, and *Cibicidoides bembix kasahstanicus* (Netskaya, 1948; Eremeeva and Belousova, 1961; Subbotina, 1964; Marinov et al., 2014). Such a similarity implies the paleogeographic connection between epicontinental seas of the East European Platform and the southern part of the West Siberian basin. The increase in the share of European benthic foraminiferal species (up to >55% of the total assemblage) in upper Maastrichtian sediments of the Gan'kino Formation in the south Trans-Urals region was previously noted in (Beniamovsky, 2005).

Summing up the analysis of composition of the benthic foraminiferal assemblage from Member 11, one should emphasize the following important differences from upper Maastrichtian assemblages from the Nikolaevskoe Formation studied in sections near the settlement of Teplovo of the Novyi Buras district and the settlement of Klyuchi of the Bazarny Karabulak district of Saratov oblast (Alekseev et al., 1999) and assemblages from the Radishchevo Formation in sections of the Volga River right bank near the town of Vol'sk and the settlement of Vishnevoe of the Petrovsk district (Olfer'ev et al., 2009a, 2009b, 2014). In the above-mentioned sections, benthic foraminiferal paleocoenoses are largely represented by anomalinids, ataxophragmiids, *Bolivinoides* species, and praebuliminids, accompanied by rare planktonic keeled glo-

[1] Bold indicates the most frequent species of paleobiogeographic and stratigraphic significance.

Plate II

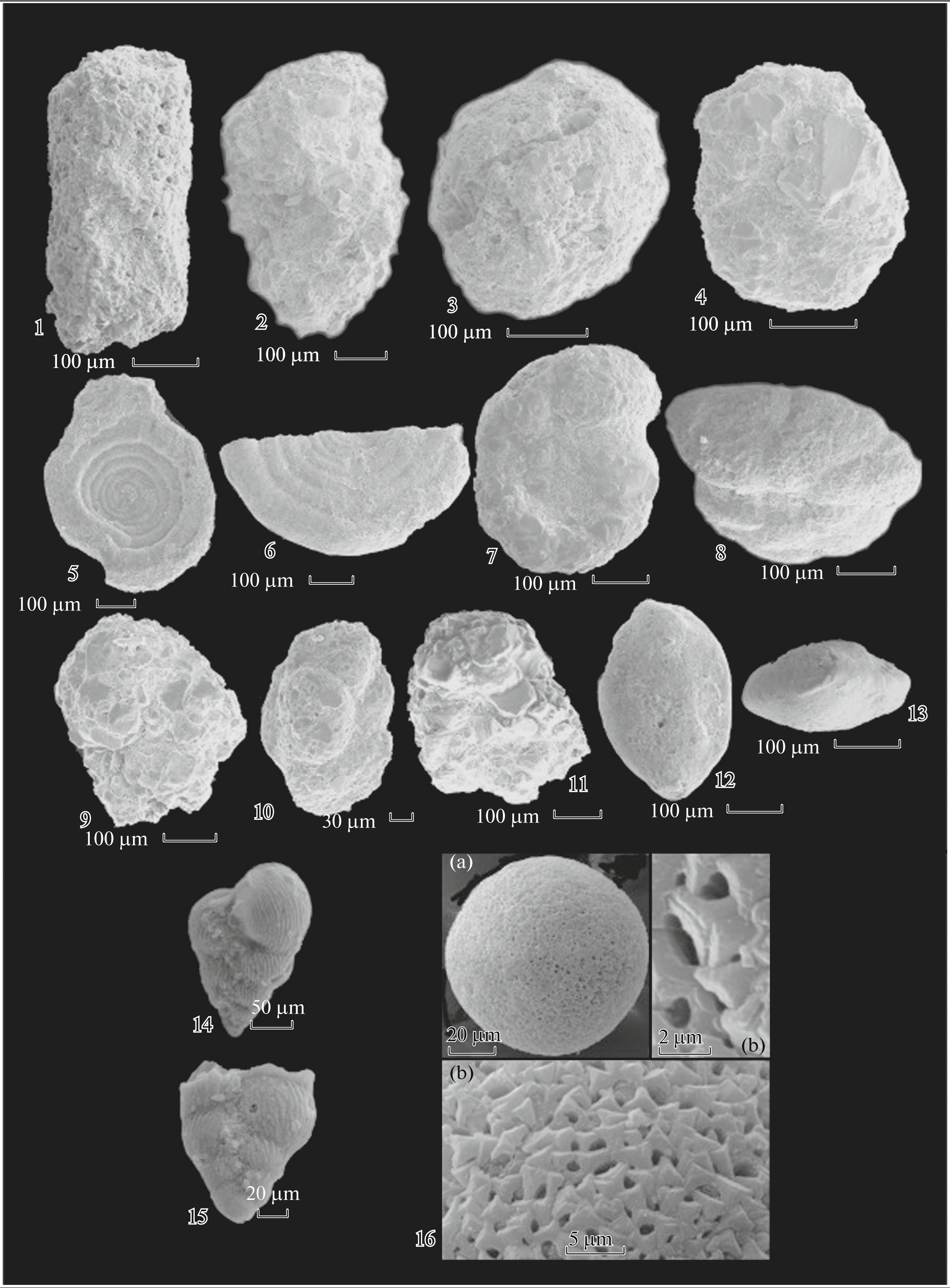
1
100 μm
2
100 μm
3
100 μm
4
100 μm
5
100 μm
6
100 μm
7
100 μm
8
100 μm
9
100 μm
10
30 μm
11
100 μm
12
100 μm
13
100 μm
14
50 μm
15
20 μm
16
(a)
20 μm
2 μm
(b)
(b)
5 μm

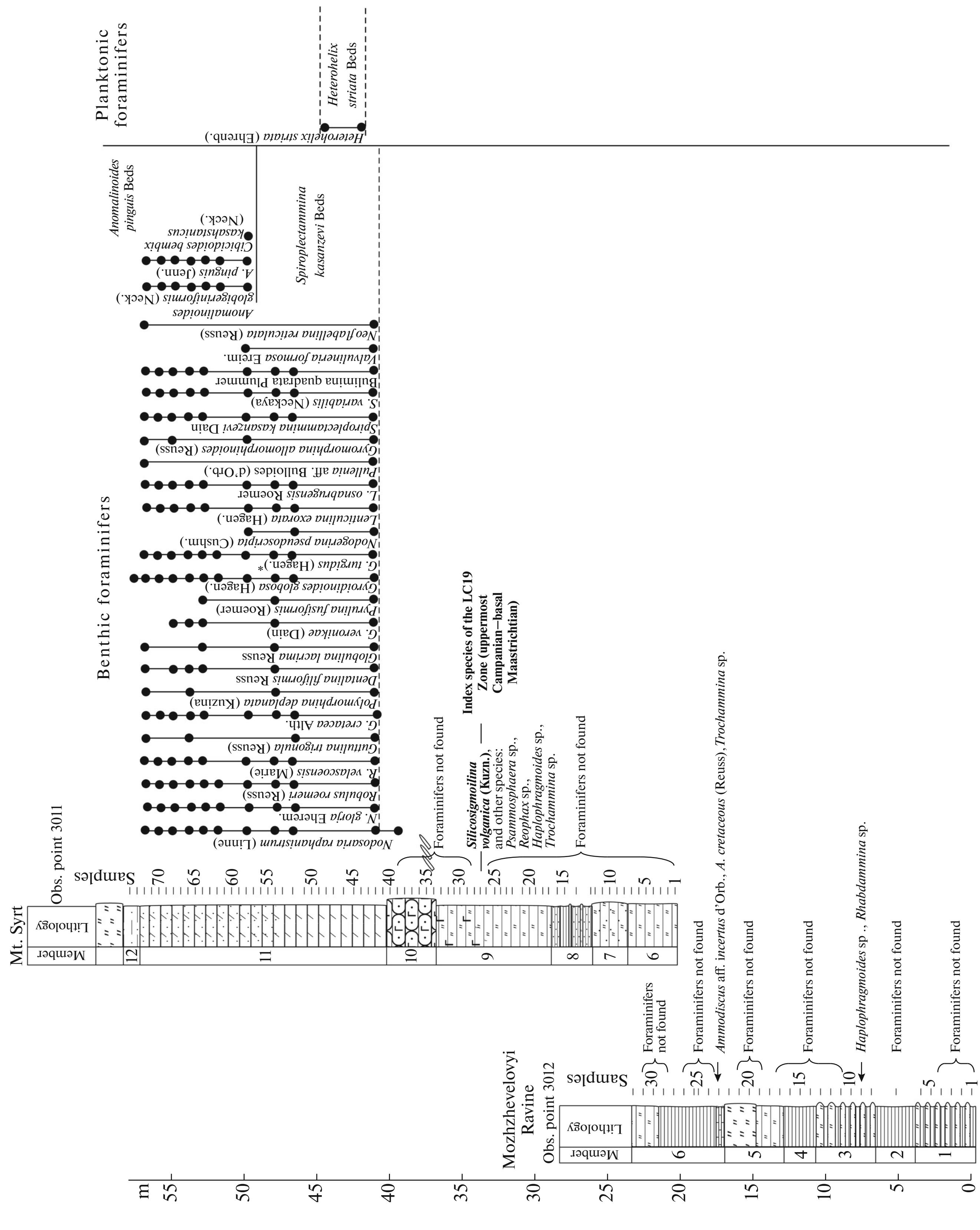

Fig. 4. Benthic and planktonic foraminifers in the Nizhnyaya Bannovka section (distribution, assemblages, and assumed age).

botruncanids, while carbonate clays of Member 11 in the Mount Syrt section are characterized by an absolutely different biocoenosis. It includes single planktonic (planispiral *Globigerinelloides* and biserial *Heterohelix* representatives) and benthic (spiroplectamminids, nodosariids, polymorphinids, discorbids, and buliminids) foraminifers. Such a composition of the foraminiferal assemblage indicates strong differentiation of water masses in the Late Cretaceous basin of the Saratov region (Volga River right bank).

Radiolarians

Four radiolarian assemblages covering different stratigraphic units are defined in the Nizhnyaya Bannovka section (Fig. 5, Plate IV).

The Prunobrachium mucronatum–Lithostrobus turitella Beds of the middle Campanian are established to correspond to Members 1–7 (Samples 3012/3, 3012/7, 3012/9, 3012/11, 3012/15, 3012/23, 3012/27, 3011/2–3011/7, 3011/9, and 3011/11). The characteristic species of this assemblage are *Phaseliforma carinata* Pessagno, *Crucella crux* (Lipman), *Orbiculiforma campbellensis* Pessagno, *O. monticelloensis* Pessagno, O. *sacramentoensis* Pessagno, *O. volgensis* (Lipman), *Prunobrachium boreale* Vishnevskaya, *P. kozlovae* Vishnevskaya, *Patulibracchium petroleumensis* Pessagno, ***Prunobrachium mucronatum* (Lipman)**, *P. angustum* (Lipman), *P. crassum* (Lipman), *P. concentricum* (Lipman). *P. ornatum* (Lipman), *P. sibiricum* (Lipman), *Dictyomitra striata* Lipman, ***Lithostrobus turitella* Lipman**, and *Stichomitra manifesta* Foreman.

The Prunobrachium articulatum Beds (upper part of the upper Campanian) are defined higher in the section in Members 8 and 9 (Samples 3011/12–3011/16, 3011/19, 3011/26, 3011/27, and 3011/28). The characteristic species of their radiolarian assemblage are *Phaseliforma carinata* Pessagno, *Crucella crux* (Lipman), *Orbiculiforma campbellensis* Pessagno, *O. monticelloensis* Pessagno, *O. sacramentoensis* Pessagno, ***Prunobrachium articulatum* (Lipman)**, *P. boreale* Vishnevskaya, *P. kozlovae* Vishnevskaya, *Pseudobrachium trilobatum* Vishnevskaya, *P. gracilis* Vishnevskaya, *Dictyomitra andersoni* Campbell et Clark, *Archaeodictyomitra regina* (Campbell et Clark), *Theocampe apicata* Foreman, and *Xitus grandis* (Campbell et Clark).

Previously, Kazintsova (2000) established in the Nizhnyaya Bannovka section the upper Campanian radiolarian assemblage with *Prunobrachium articulatum*. The study of Sample 5 (from the collection by A.G. Olfer'ev and L.I. Kazintsova; Vishnevskaya et al., 2014) from the uppermost part of the Pudovkino Formation (Ovechkina, 2007) represented by alternating slightly siliceous marlstones and light gray opokas revealed abundant skeletons of the late Campanian species *Prunobrachium articulatum* (Lipman), accompanied by *Prunobrachium crassum* (Lipman), *P. angustum* (Lipman), *Crucella crux* (Lipman), and *Xitus grandis* (Campbell et Clark), which confirm the late Campanian age of this assemblage.

The Rhombastrum Beds are defined in the terminal part of Member 9 (Sample 32), where they are characterized by two distinct features: total disappearance of all forms constituting the preceding assemblage and the appearance of representatives of the genus *Rhombastrum*. This assemblage is considered to be transitional between the Campanian and Maastrichtian radiolarian communities.

The fourth, upper Maastrichtian, Spongurus marcaense–Tholodiscus densus Assemblage characterizes presumably the basal part of the Lokh Formation (Samples 3011/43–3011/53). Its characteristic species are represented by *Rhombastrum* sp., *Spongurus marcaensis* Pessagno, *S. splendiarmatum* (Clark et Campbell), *Dictyomitra andersoni* Campbell et Clark, *Archaeodictyomitra regina* (Campbell et Clark), *Orbiculiforma australis* Pessagno, *Orbiculiforma renillaeformis* (Campbell et Clark), and *Tholodiscus densus* (Kozlova).

It should be noted that the assemblage from the Spongurus marcaense–Tholodiscus densus Beds is close in its composition to the Spongurus marcaense–Rhombastrum russiense Assemblage from the terminal part of the Sukhodol Formation in northern Rostov oblast corresponding to the transitional Campanian–Maastrichtian interval of the LC19 benthic foraminiferal zone (Beniamovsky et al., 2012). In this assemblage, noteworthy is *Orbiculiforma renillaeformis*, the index species of the synonymous assemblage from the O. renillaeformis Beds of the Nalitovo Formation in southwestern Volgograd oblast, which are correlative with the uppermost part of the LC19 Zone together with the lower Maastrichtian dinocyst Canningia microreticulata Beds (Aleksandrova et al., 2012). The O. renillaeformis Beds are defined in the lower Maastrichtian Zhuravlevo Formation near Kustanai in the Tobol region (Amon, 1990), the age of which is confirmed by findings of *Belemnella* ex gr. *sumensis* Jel. and *B. sumensis praearkhangelskii* Naid. rostra (Naidin, 1990). The O. renillaeformis Zone is also recognizable in the lower Maastrichtian sections of California (Pessagno, 1976).

The Prunobrachium articulatum Beds are indicative of the upper Campanian interval in sections of the East European Platform, West Siberia, and Subpolar Urals (*Prakticheskoe*..., 1999; Vishnevskaya, 2001), while the Maastrichtian interval is determined by the appearance of high-conical cainotypic dictyomitrids and the first *Spongurus marcaensis*, *Orbiculiforma renillaeformis*, etc. (Vishnevskaya, 2009, 2010). Thus, according to radiolarians, the Campanian–Maastrichtian boundary in the Nizhnyaya Bannovka section is placed in the upper part of Member 9 between Samples 3011/28 and 3011/32, which is consistent with its position substantiated by benthic foraminifers (LC19 Zone).

Plate III. Benthic foraminifers from the Nizhnyaya Bannovka section (Member 11). (1) *Spiroplectammina kasanzevi* Dain, Sample 3011/49; (2, 3*) Nodosaria raphanistrum* (Linne), Sample 3011/49; (4, 5) *N. gloria* Ehrem, Samples 3011/72 and 3011/62, respectively; (6) *Darbyella* sp., Sample 3011/54; (7) *Lenticulina exorata* (Hagen.), Sample 3011/58; (8, 9) *Robulus* sp., Samples 3011/70 and 3011/58, respectively; (10) *Planulina* sp., Sample 3011/58; (11) *Guttulina trigonula* (Reuss), Sample 3011/49; (12) *Pyrulina fusiformis* (Roemer), Sample 3011/49; (13) *Vaginlulinopsis* sp., Sample 3011/54; (14, 15) *V. trilobatus* (d'Orb.), Samples 3011/58 and 3011/66, respectively; (16) *Gyroidinoides globosus* (Hagen.), Sample 3011/52; (17) *Pullenia* aff. *bulloides* (d'Orb.), Sample 3011/49; (18) *Gyromorphina allopmorphinoides* (Reuss), Sample 3011/62; (19–22) *Anomalinoides globigeriniformis* (Neck.): (19) dorsal view, Sample 3011/62; (20) umbilical view, Sample 3011/62; (21, 22) lateral view, Samples 3011/64 and 3011/68, respectively; (23–25) *Anomalinoides pinguis* (Jenn.): (23) dorsal view, Sample 3011/58; (24) umbilical view, Sample 3011/64; (25) lateral view, Sample 3011/64; (26) *Bulimina quadrata* Plummer, Sample 3011/54; (27) *Nodogenerina* sp., Sample 3011/54; (28, 29) *N. pseudoscriptus* (Cushm.), Samples 3011/54 and 3011/52, respectively.

Nannofossils

The nannofossil assemblage from Member 11 (Samples 3011/44–3011/71) is represented by *Effellithus turriseiffeli*, *Micula concava*, and *M. decussata*. The assemblage includes species belonging to several groups (Plate V) (Vishnevskaya et al., 2012): (1) *Arkhangelskiella specillata* Vekshina and *Broinsonia parca parca* (Stradner), which are distributed in the lower Campanian–lower Maastrichtian interval; (2) *Discorhabdus ignotus* (Górka) and *Dodekapodorhabdus noelinae* Perch-Nielsen, characterizing mostly the upper Campanian–Maastrichtian sediments; (3) *Eiffellithus turriseiffeli* (Deflandre in Deflandre et Fert), *Kamptnerius magnificus* Deflandre, *Micula concava* (Stradner in Martini et Stradner), *Micula decussata* Vekshina, and *Prediscosphaera bukryi* Perch-Nielsen, which appear in the uppermost Campanian and are traceable to the Maastrichtian (Ovechkina, 2007). Member 11 (Sample 3011/60) yielded also *Kamptnerius magnificus* Deflandre, which is distributed in the Cenomanian–Maastrichtian interval.

Calcareous Dinocysts

The basal part of Member 11 (Sample 3011/44) contains *Pithonella*-type calcareous dinocysts (Plate II) attributed to *Pithonella globosa* Futterer, 1984, which is distributed in the upper Maastrichtian–Danian sediments of the Angola Basin in the Atlantic Ocean and on the Kerguelen Plateau and Wombat Plateau in the Indian Ocean (Fütterer, 1984; Vishnevskaya, 2015).

Calcareous dinocysts found in the Nizhnyaya Bannovka section are externally similar to *Pithonella krasheninnikovi* Bolli and morphotype of *Orthopithonella gustafsoni* Bolli from the upper Maastrichtian sediments of the Weddell Sea in Antarctica, but are distinguished from them by their regular spherical shapes and smaller crystals (over a hundred crystals per diameter versus up to 50 in *O. gustafsoni*). According to (Streng et al., 2004), the presence of a small archeopile in such calcareous dinocysts reflects a warm climatic episode.

Consequently, the find of calcareous dinocyst *Pithonella globosa* Futterer allows host sediments to be dated to the late Maastrichtian (not older) and implies a warm episode during deposition of calcareous clays (Fütterer, 1984).

Thus, the following data on different groups of macro- and microfossils from the upper Campanian–lower Maastrichtian Nizhnyaya Bannovka section are in essence new: (1) information on the *belemnite* assemblage, which allows glauconite sandstones (Member 10) to be attributed to the upper Campanian Belemnitella langei Zone; (2) data on benthic foraminifers, which made it possible to define for the first time the Spiroplectammina kasanzevi and Anomalinoides pinguis beds in the Maastrichtian interval of the Saratov region; (3) recognition of four bed-ranked stratigraphic units with *radiolarians*, three of which (middle Campanian, transitional Campanian–Maastrichtian, and upper Maastrichtian) were never defined before; (4) data on upper Maastrichtian *calcareous dinocysts* (Pithonella globosa Beds).

MAGNETOSTRATIGRAPHY

Petromagnetic and magnetic–mineralogical investigations included the study of magnetic susceptibility (K) and its anisotropy (AMS), measurements of natural remanent magnetization ($\mathbf{J_n}$), experiments on magnetic saturation with determination of remanent saturation magnetization ($\mathbf{J_{rs}}$) and remanent coercivity ($\mathbf{H_{cr}}$), and thermomagnetic analysis (TMA). K was measured on a FK1-FB kappabridge; $\mathbf{J_n}$ was measured on a JR-6 spinner magnetometer and 2G-Eneterprices cryogenic magnetometer (at the Institute of Physics of the Earth (IFZ), Russian Academy of Sciences, Moscow); TMA was conducted of a TAF-2 thermal analyzer of fractions ("magnetic balance"). The Anisoft 4.2 program was used for the AMS analysis. Selected samples from different rock lithotypes were investigated on the TESCAN VEGA II in the Borok Observatory of IFZ.

The composite section is differentiated with respect to petromagnetic properties (Fig. 6). Against the background of low-magnetization siliceous–terrigenous and carbonate–terrigenous rocks (K = 2–18 × 10^{-5} SI, $\mathbf{J_n}$ = 0.03–0.7×10^{-3} A/m), glauconite sand (Member 10) is characterized by elevated K values (34–58×10^{-5} SI), which is explained by properties of glauconite, which is a strongly paramagnetic mineral. The upper part of the member includes a level with anomalously high $\mathbf{J_n}$ values (1.8–3.5×10^{-3} A/m). The K values in siliceous–terrigenous Members 1–9 are unambiguously explained by concentrations of

Plate III

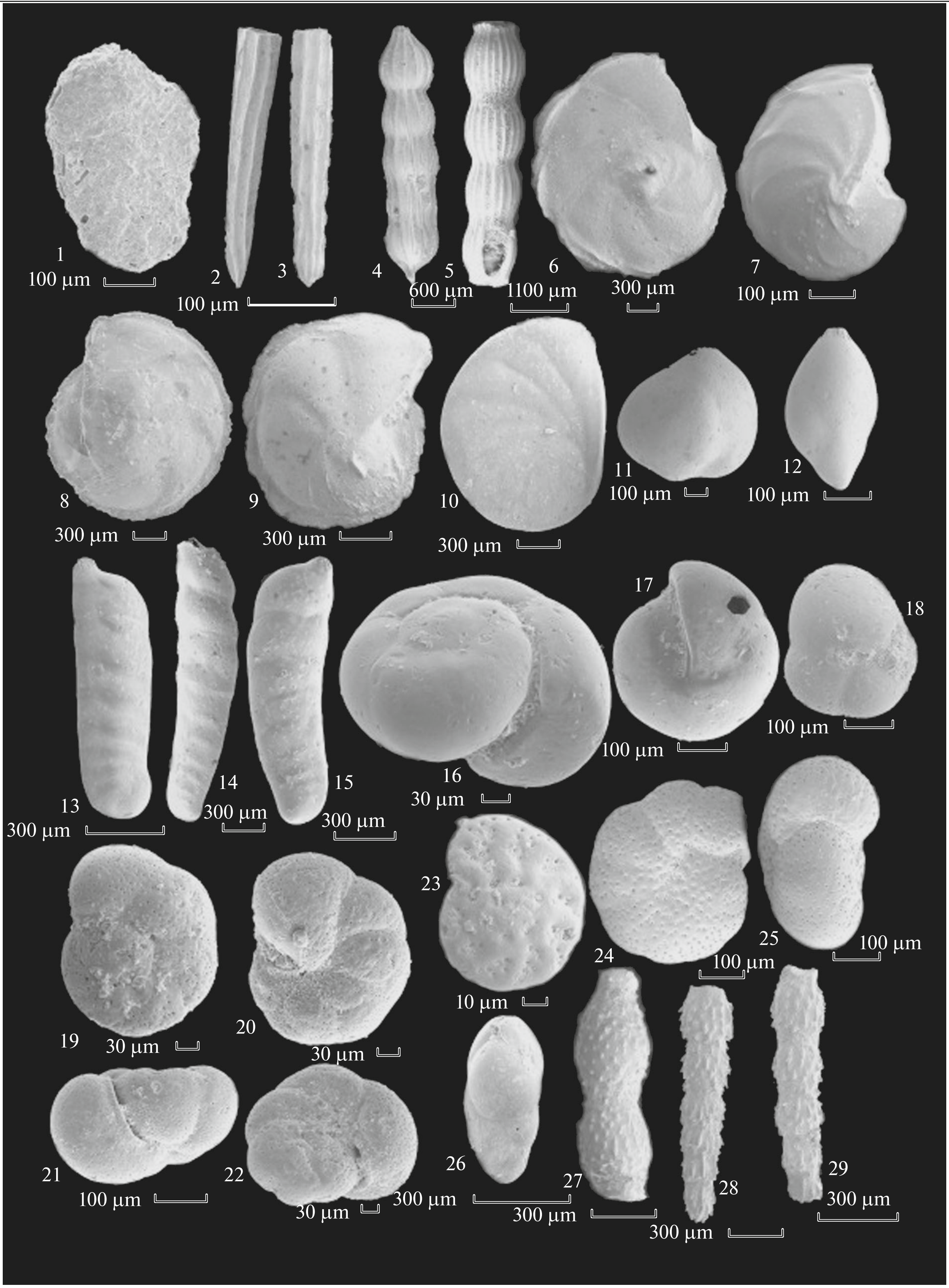
1
100 μm
2
3
100 μm
4
5
600 μm
6
1100 μm
300 μm
7
100 μm
8
300 μm
9
300 μm
10
300 μm
11
100 μm
12
100 μm
13
300 μm
14
300 μm
15
300 μm
16
30 μm
17
100 μm
18
100 μm
19
30 μm
20
30 μm
23
10 μm
24
100 μm
25
100 μm
21
100 μm
22
30 μm
26
300 μm
27
300 μm
28
300 μm
29
300 μm

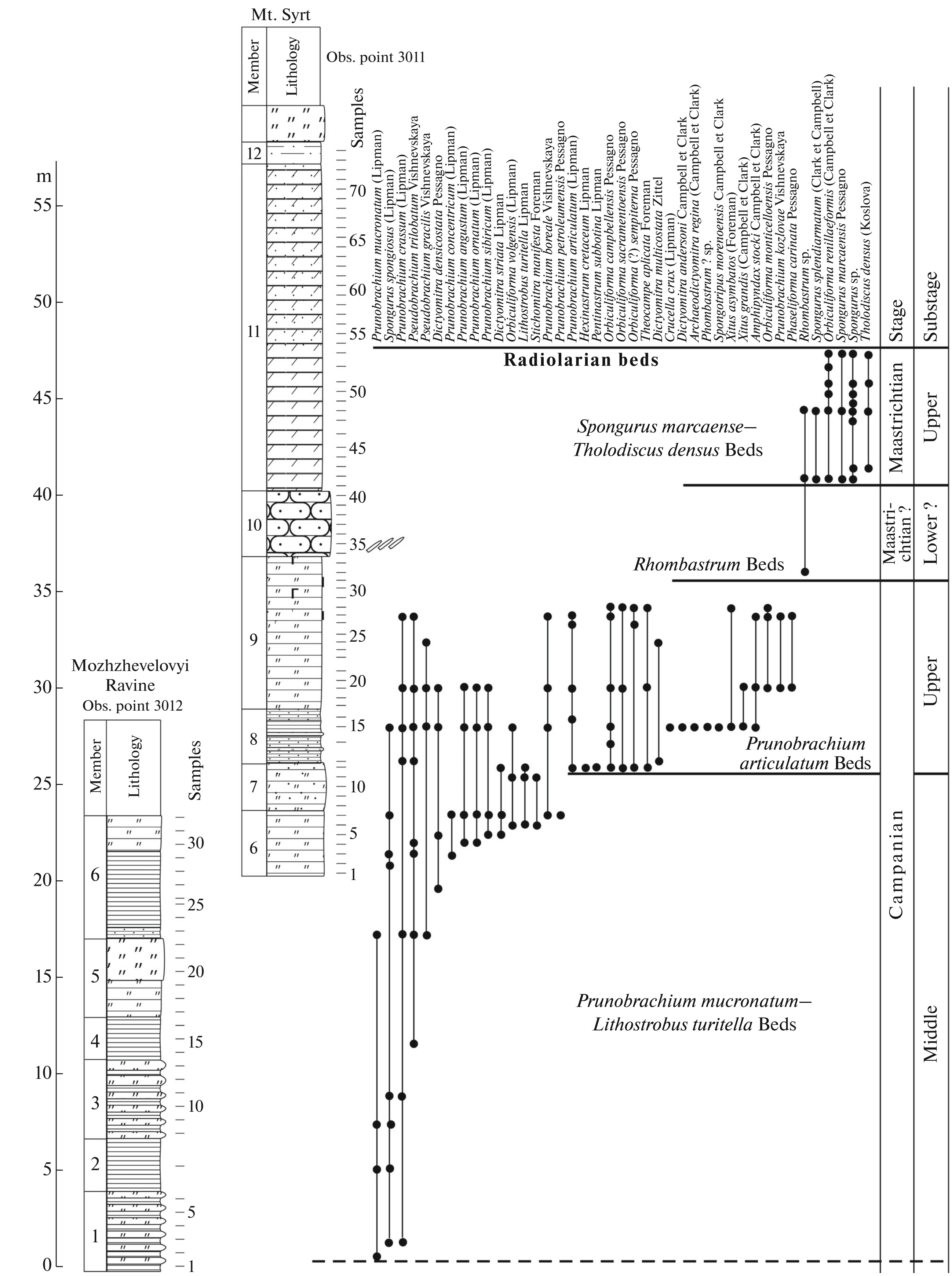

Fig. 5. Radiolarians in the Nizhnyaya Bannovka section (distribution, assemblages, and assumed age).

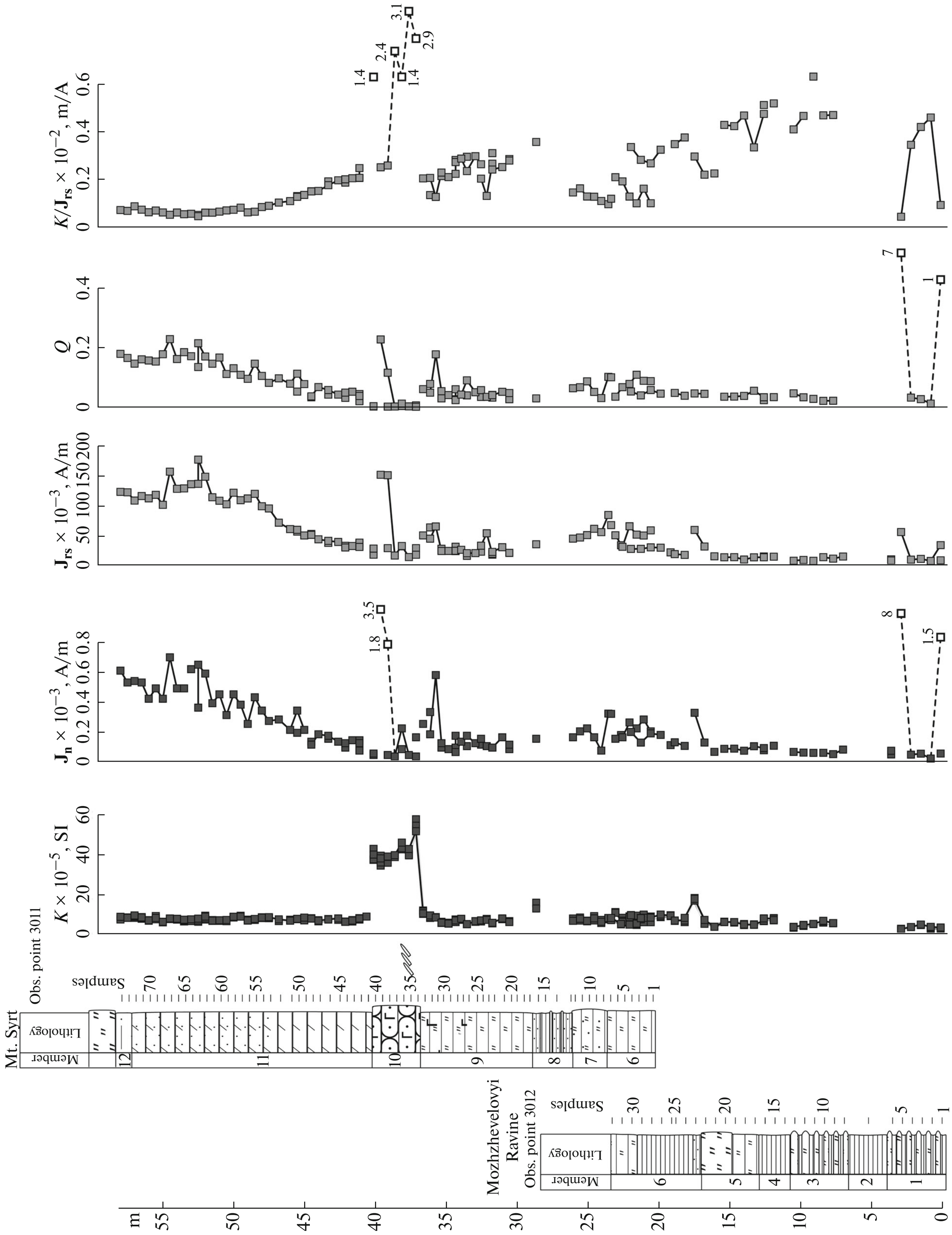

Fig. 6. Petromagnetic record of the Campanian–Maastrichtian Nizhnyaya Bannovka section.

clayey particles in opokas reaching local maxima in siliceous clays (3–5×10^{-5} SI) and rare intercalations of silty–sandy clays (18×10^{-5} SI). Carbonate–terrigenous Members 11–12 demonstrate no notable K variations, although the $K/\mathbf{J}_{\mathbf{rs}}$ parameter exhibits a distinct tendency toward its decrease, while $\mathbf{J}_{\mathbf{n}}$, Q (Koenigsberger parameter equal to ratio between $\mathbf{J}_{\mathbf{n}}$ and inductive magnetization), and $\mathbf{J}_{\mathbf{rs}}$ values are characterized by a similarly remarkable trend of their upward increasing values (Fig. 6). This is accompanied by the regular $\mathbf{H}_{\mathbf{cr}}$ increase from 35 to 45 mT.

The analysis of magnetic saturation in examined samples reveals the soft magnetic phase: $\mathbf{J}_{\mathbf{rs}}$ is acquired in fields up to 100 mT and destroyed at 20–40 mT (Fig. 7a). Such a situation is characteristic of finely dispersed magnetite. According to TMA curves (plots of derivatives are poorly informative since they reflect mostly instrumental noises, which are comparable with the signal from magnetization of samples), magnetite is difficult to identify. Nevertheless, its presence is evident from a sight bend in TMA curves near the Curie temperature of Fe_3O_4 of ~580°C in different rock types, for example, in Samples 3012/5 and 3011/61 (Fig. 7b). Moreover, this bend disappears completely after the second heating, which may indicate, together with the substantial loss of magnetization, the finely dispersed state of Fe_3O_4 entirely oxidized during the first heating session. The TMA curves reflect more distinctly a ferromagnetic mineral with the Curie temperature of ~700°C and higher (Fig. 7b), which implies, combined with soft magnetization of samples, the presence of native Fe (Pechersky et al., 2011). The results of the microprobe analyses show the prevalence of Fe, Fe–Ni, or Fe–Cr–Ni flakes and magnetite spherules in the ferromagnetic fraction (Fig. 7d). The chemical composition (Fe, Ni, Cr), submicron size, and shape of particles (flakes, spherules) are characteristic of meteoritic dust and combined with other results of the magnetic mineral analysis provide grounds for admitting extraterrestrial magnetite and iron as being the probable carriers of $\mathbf{J}_{\mathbf{n}}$ in the section.

AMS is highly variable in different rock types. Carbonate–terrigenous Members 11 and 12 are characterized by the distribution of projections of magnetic susceptibility ellipsoid axes typical of sediments deposited in low-energy hydrodynamic environments: projections of short axes (*K3*) are concentrated in the center of the stereographic projection, while projections of medium (*K2*) and long (*K1*) axes are regularly distributed along its equator (Fig. 7c). Similar, although less distinct, patterns are also observable in the siliceous–terrigenous part of the section (Members 1–9) (Fig. 7c). The magnetic structure of glauconite sands (Member 10) demonstrates the elongated extension of short axes and significant deviation of the average *K3* direction from the vertical line, while *K1* projections deviate from the horizontal plane (Fig. 7c). Being combined, these observations may be interpreted as resulting from the influence of strong bottom currents oriented in the SW–NE direction or suffosion processes in poorly consolidated sandstone (Lagroix and Banerjee, 2004). The last scenario is unlikely since external features of suffosion are missing and overlying carbonate–terrigenous Members 11 and 12 are characterized by AMS indicating unmixed rocks (Fig. 7c).

The *F–L* diagrams for the carbonate–terrigenous part of the section imply the flat shape of ferromagnetic particles (Fig. 7c). This effect is provided by aggregated extraterrestrial dust on clayey particles. In opokas and glauconite sands, the *F–L* diagrams reveal variably shaped ferromagnetic grains (Fig. 7c).

Paleomagnetic investigations were conducted in accordance with the standard technique (Molostovskii and Khramov, 1997) consisting in the measurement of $\mathbf{J}_{\mathbf{n}}$ values in samples 2 × 2 × 2 cm in size (four cubic specimens were preliminarily cut from each oriented sample) on the JR-6 spinner magnetometer after a series of several successive cleaning sessions by a variable geomagnetic field mostly up to 50–100 mT (step of 5 mT) on the LDA-3 AF device at temperatures ranging from 100 to 550°C (step of 50°C) in a furnace designed by Aparin. Possible phase transformations of minerals during heating were controlled by measuring K in samples after each thermal cleaning session. In most samples, stable magnetization components were revealed owing to cleaning by the variable geomagnetic field. Only glauconite-bearing samples were subjected to both types of demagnetization. Paleomagnetic investigations of samples taken from most levels were repeated on the cryogenic (SQUID) 2G-Enterprices magnetometer at IFZ, and the results of these measurements on both devices demonstrate sufficient consistency (Fig. 8). The Remasoft 3.0 program was used for the component analysis.

In the carbonate–terrigenous and siliceous–terrigenous parts of the section, the characteristic $\mathbf{J}_{\mathbf{n}}$ **(ChRM)** components were defined for 68 of 88 sampled stratigraphic levels. The maximum deviation

Plate IV. Radiolarians from the Nizhnyaya Bannovka section. (1–3) *Prunobrachium mucronatum*; (4) *P. boreale* Vishnevskaya; (5, 8) *P. crassum* (Lipman); (6, 7) *P. koslovae* Vishnevskaya; (9) *Stylotrochus hexacanthus* Lipman; (10) *Phaseliforma concentrica* (Lipman); (11) *Crucella aster* (Lipman); (12) *Spongotripus morenoensis* Campbell et Clark; (13) *Tholodiscus densus* (Koslova); (14) *T. fresnoensis* (Foreman); (15, 16) *Rhombastrum* sp.; (17) *Stylotrochus octancathus* Lipman; (18) *Archaeospongoprunum stocktonensis* Pessagno; (19) *A. hueyi* Pessagno; (20) *Dictyomitra densicostata* Pessagno; (21) *D. andersoni* (Campbell et Clark); (22) *Xitus asymbathos* Foreman; (23) *X. grandis* (Campbell et Clark); (24) *Stichomitra carnegiense* (Campbell et Clark); (25) *Lithostrobus* sp.; (26) *Amphipyndax* sp. (1, 4, 8) Sample 3011/4; (2, 3, 6, 10, 11, 14, 20) Sample 3011/13; (5, 7, 12, 13, 15, 16, 17, 22) Sample 3011/14; (9, 19, 25) Sample 3011/27; (18, 21, 23, 24, 26) Sample 3011/28. Scale bar is 100 μm.

Plate IV

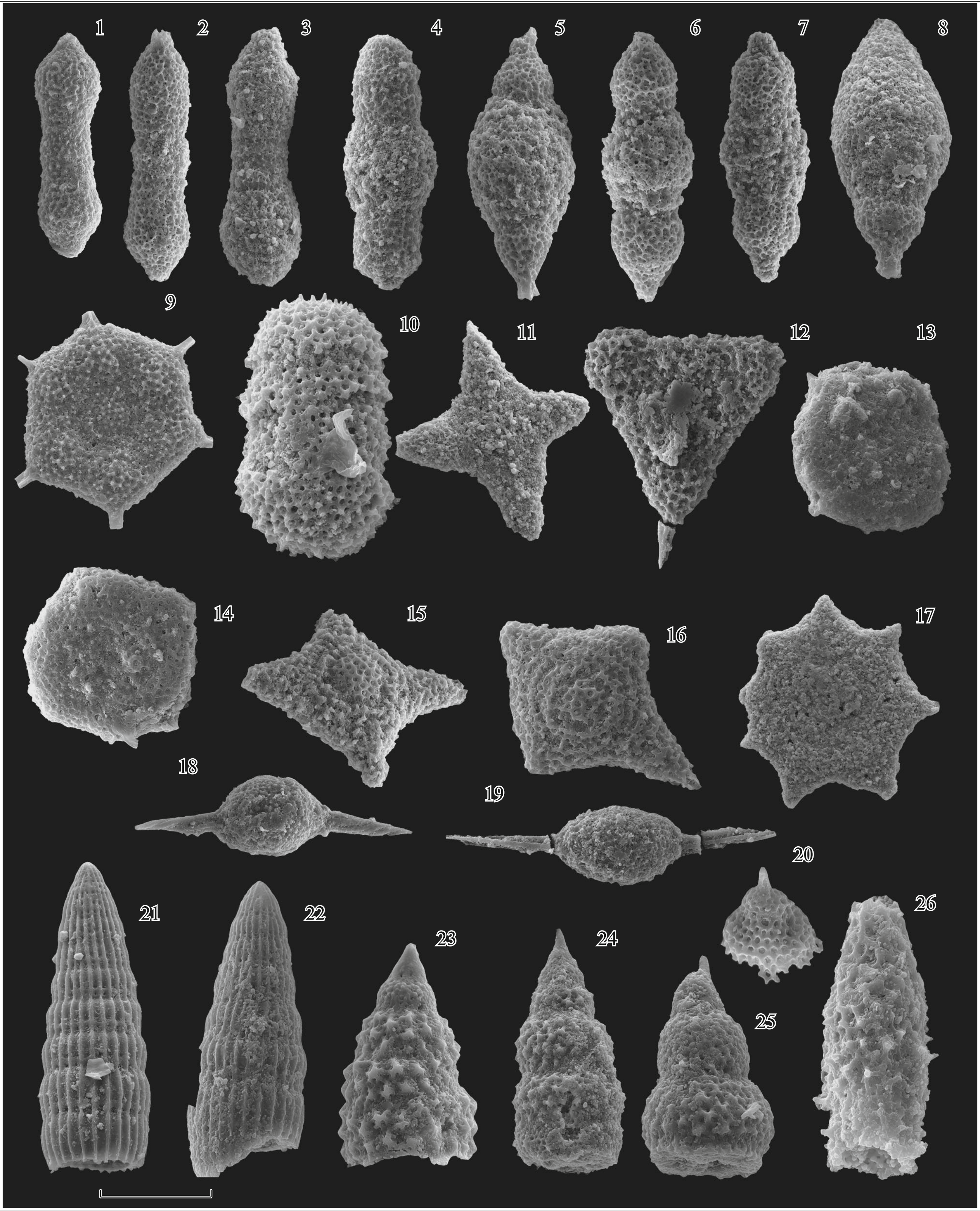

angle (the accuracy characterizing the approximation of data on a straight line in the Zijderveld diagram) never exceeded 15° (Fig. 9). Projections of paleomagnetic vectors obtained at 65 levels, which are grouped in the northern rhumbs of the lower hemisphere (Fig. 10a), are interpreted as reflecting normal polarity (*N*) of the geomagnetic field. The single level in the carbonate clay sequence of Member 11 and two levels in siliceous rocks (the base of Member 1) yielded directions characteristic of reversed polarity (*R*). In 20 samples, **ChRM** was undetectable.

Glauconite sands from Member 10 are informative with respect to their paleomagnetic properties. In these sediments, **ChRM** of reversed polarity is defined only in highly magnetic ($\mathbf{J_n}$ = 1.8–3.5×10^{-3} A/m) varieties, while in all other samples (except for Sample 3011/40 from the uppermost part of Member 10), the $\mathbf{J_n}$ components are regularly projected onto the upper hemisphere (Fig. 10a). Regardless of the cleaning type and measuring device, the paleomagnetic results are well consistent between each other (Figs. 8, 10b); therefore, despite extremely low intrasample and intrabed precision parameters (Fig. 10a), we believe that they are determined by the field of reversed polarity. It should also be noted that the possibility of obtaining paleomagnetic information from glauconite was recently substantiated in (Lurcock and Wilson, 2013).

Thus, the paleomagnetic record in the Nizhnyaya Bannovka section demonstrates three magnetic zones: lower, of normal polarity (N_1) corresponding to Members 1–9; middle, of reversed polarity (*R*) comprising Member 10, except for its uppermost part; upper, of normal polarity (N_2) characterizing the uppermost part of Member 10 and Members 11 and 12 (Fig. 10). Theoretically, *R* intervals at the base of Member 1 (Samples 3012/1 and 3012/2) and in the upper part of Member 11 (Sample 3011/66) may be autonomous zones, but this conclusion is as yet groundless, since they are characterized by one or two samples, while the magnetic zone should be substantiated by samples from at least three levels. Lacunes in the paleomagnetic record concede the existence of narrow intervals with polarity of the opposite sign against the background of prevalent polarity in the section, but their appearance cannot change the inference on the three-member structure of the paleomagnetic record in the section under consideration.

The impossibility of field tests (the reverse test is impossible because of unfitness of data on the presumable presence of the *R* zone in glauconite sand for calculation of paleomagnetic statistics, while prerequisites for tests of folds, conglomerates, and others are missing) is not an obstacle for interpretation of magnetic polarity data, since there are several features which may be used in magnetostratigraphic investigations for substantiating old $\mathbf{J_n}$ age (Guzhikov, 2013a; etc.).

(1) Intervals of the same sign of polarity derived from ChRM directions are regularly grouped through the section forming large *N* or *R* magnetic zones (Fig. 10).

(2) The sign of polarity demonstrates no dependence on lithology of sediments: the reverse polarity magnetozone *R* encompasses partly the member of glauconite sandstone, while its uppermost part belongs to the overlying normal polarity *N* magnetozone (Fig. 10).

(3) The average paleomagnetic directions obtained for the Campanian interval of the Nizhnyaya Bannovka section are statistically similar to their counterparts in coeval sediments of the Vol'sk area (Figs. 11a, 11b), where the old $\mathbf{J_n}$ age is substantiated by different data, including positive results of the reverse test (Guzhikova and Bagaeva, 2013). The insignificant (1.3°) excess of the angular distance over the statistical error in comparison of average ChRM values obtained for the upper Maastrichtian sediments in the Nizhnyaya Bannovka section and Campanian strata of the Vol'sk area (Fig. 11c) is likely explained by motion of lithospheric plates during the Maastrichtian Age.

(4) The entire section exhibits both the features characteristic of orientational (post-orientational) magnetization and those atypical of chemical $\mathbf{J_n}$: low values of the *Q* factor (fractions of a unit) and low paleomagnetic interbed precision parameter (11–21) (Fig. 10a). The main magnetization carrier in the section represented by extraterrestrial dust, the presence of which is evident from the magnetic saturation, TMA, and microprobe data (Fig. 7), is allogenic by nature.

(5) The significant scatter of paleomagnetic vectors in the member of glauconite sandstones (Fig. 10a) is expectable since glauconite indicates low sedimenta-

Plate V. Calcareous nannofossils from the Nizhnyaya Bannovka section (Member 11). (1) *Chiastozygus* sp., distal view, Barreman–Maastrichtian, Sample 3011/71; (2) *Staurolithites* sp., lateral view, Oxfordian–Maastrichtian, Sample 3011/50; (3) *Cribrosphaerella ehrenbergii* (Arkhangelsky), distal view, Campanian–Maastrichtian, Sample 3011/50; (4) *Discorhabdus ignotus* (Górka), distal view, Albian–Maastrichian, Sample 3011/44; (5) *Prediscosphaera arkhangelskyii* (Reinhardt), distal view, Coniacian–Maastrichtian, Sample 3011/44; (6) *Prediscosphaera bukryii* Perch-Nielsen, distal view, Campanian–Maastrichtian, Sample 3011/44; (7) *Prediscosphaera cretacea* (Arkhangelsky), distal view, upper Santonian–Maastrichtian, Sample 3011/71; (8) *Arkhangelskiella cymbiformis* Vekshina, distal view, Coniacian–Maastrichtian, Sample 3011/48; (9) *Arkhangelskiella specillata* Vekshina, distal view, Campanian–Maastrichtian, Sample 3011/44; (10) *Broinsonia parca parca* (Stradner), distal view, Campanian–Maastrichtian, Sample 3011/44; (11, 12) *Broinsonia* sp., Barremian–Maastrichtian, Sample 3011/44: (11) distal view, (12) proximal view; (13–17) *Kamptnerius magnificus* Deflandre, Cenomanian–Maastrichtian: (13) distal side, fragment of coccolith, Sample 3011/44; (14–17) proximal view: (14, 16, 17) Sample 3011/44, (15) Sample 3011/71; (18, 19) *Micula decussata* Vekshina, upper Coniacian–Maastrichtian, Sample 3011/44; (20) *Micula* sp., Santonian–Maastrichtian, Sample 3011/44.

Plate V

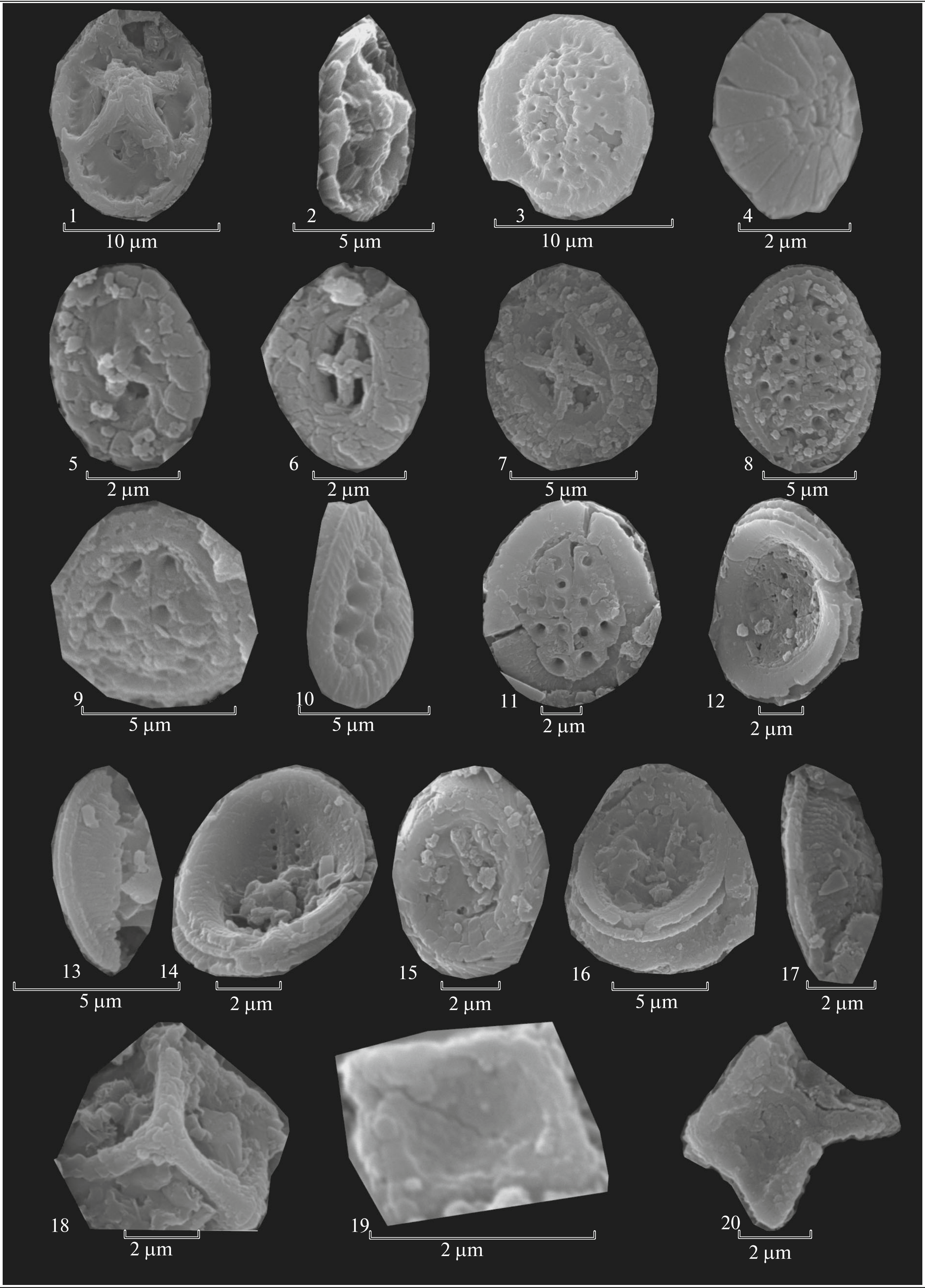
1
10 μm
2
5 μm
3
10 μm
4
2 μm
5
2 μm
6
2 μm
7
5 μm
8
5 μm
9
5 μm
10
5 μm
11
2 μm
12
2 μm
13
14
5 μm
2 μm
15
2 μm
16
5 μm
17
2 μm
18
2 μm
19
2 μm
20
2 μm

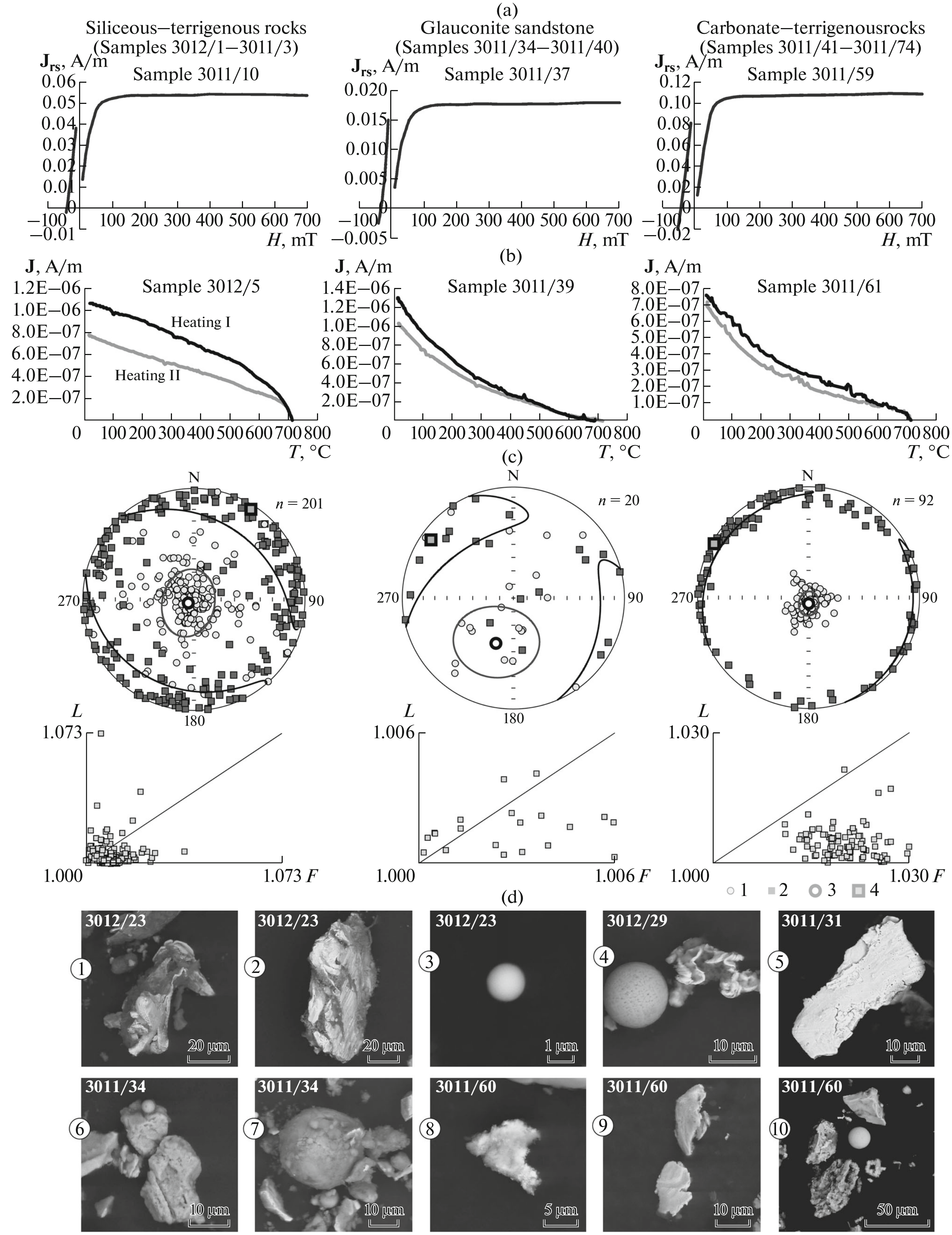
(a)
Siliceous–terrigenous rocks (Samples 3012/1–3011/3)
Glauconite sandstone (Samples 3011/34–3011/40)
Carbonate–terrigenousrocks (Samples 3011/41–3011/74)
Sample 3011/10
Sample 3011/37
Sample 3011/59
J_{rs}, A/m
H, mT
(b)
J, A/m
Sample 3012/5
Sample 3011/39
Sample 3011/61
Heating I
Heating II
T, °C
(c)
N
270
90
180
n = 201
n = 20
n = 92
L
F
1.073
1.006
1.030
1.000
1 2 3 4
(d)
3012/23
3012/29
3011/31
3011/34
3011/60
20 μm
1 μm
10 μm
5 μm
50 μm

Fig. 7. Results of the magnetic–mineralogical analysis. (a) Curves of magnetic saturation and destruction; (b) curves of thermomagnetic analysis (first and second heating); (c) data on anisotropy of magnetic susceptibility; stereograms of projections of long (*K1*) and short (*K3*) axes of AMS in the geographic coordinate system and diagrams *L*–*F* (*F* = *K2*/*K3*, *L* = *K1*/*K2*); (1) *K3*, (2) *K1*, (3, 4) average directions of *K3* and *K1*, respectively; (d) results of the microprobe analysis: (1) Ni–Fe; (2) Fe; (3) Fe_3O_4; (4) Fe_3O_4, Fe; (5) Ni; (6) Fe, Fe_3O_4; (7) Fe_3O_4, Fe; (8) Sn–Ni–Fe–Cu; (9) Fe, Fe–Cr–Ni; (10) Fe, Fe_3O_4.

tion rates and is formed during long exposition of the bottom, when sediment is subjected to various hydrodynamic impacts such as bottom turbulent and laminar mixing. Such factors distort the primary orientation of ferromagnetic particle in the sediment; therefore, the observed anomalously high scatter in paleomagnetic orientation should be considered as indicating the primary nature of magnetization. To the contrary, the high precision parameter of paleomagnetic vectors in glauconite sandstone would indicate secondary $\mathbf{J_n}$ origin.

Each of these features alone is only consistent with the hypothesis of old $\mathbf{J_n}$ nature, while their combina-

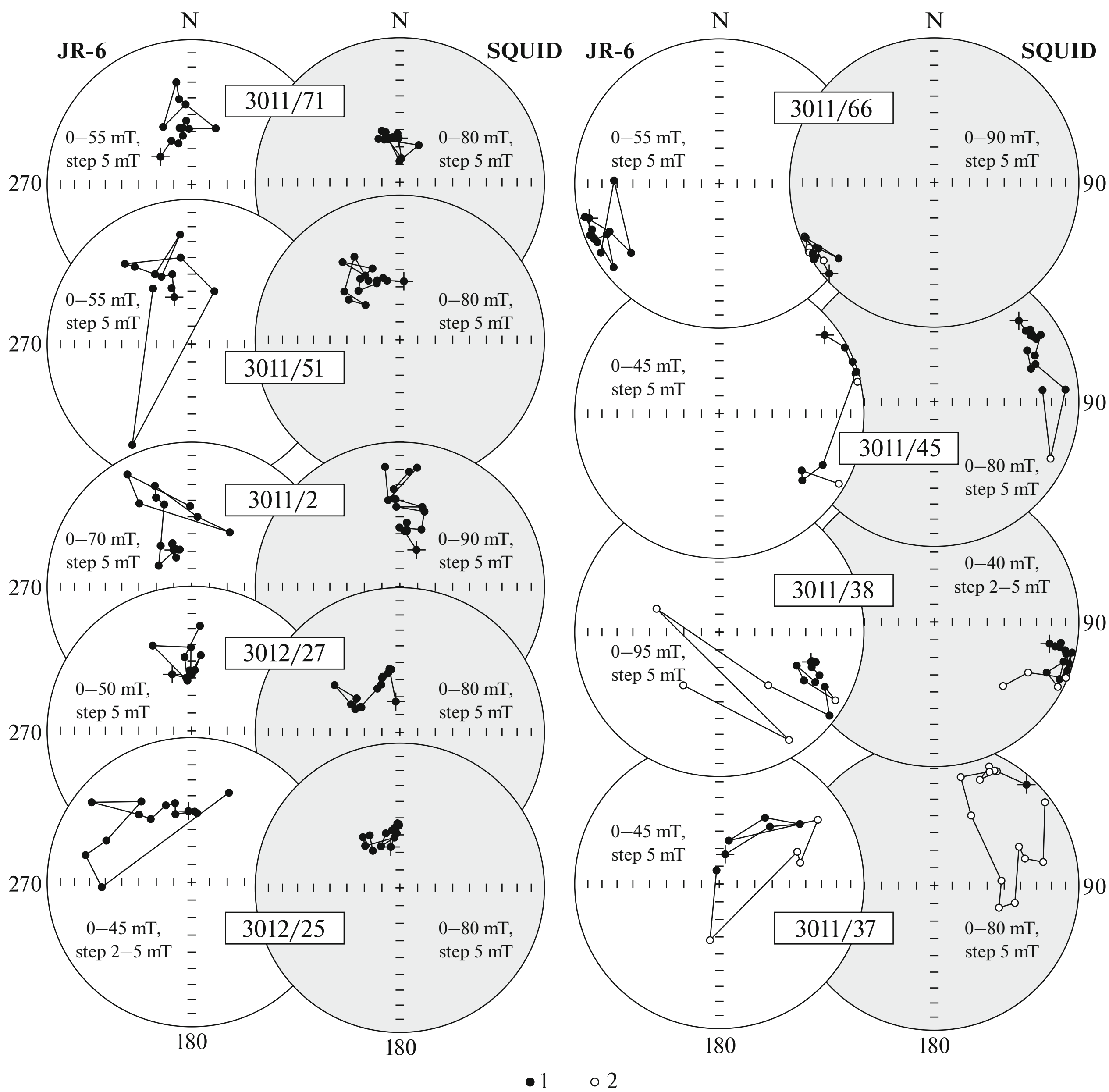

Fig. 8. Comparison of results of magnetic cleaning on the JR-6 spinner magnetometer at Saratov State University and 2G-Enterprices cryogenic magnetometer at IFZ (Moscow). (1, 2) projections of $\mathbf{J_n}$ on the lower (1) and upper (2) hemispheres.

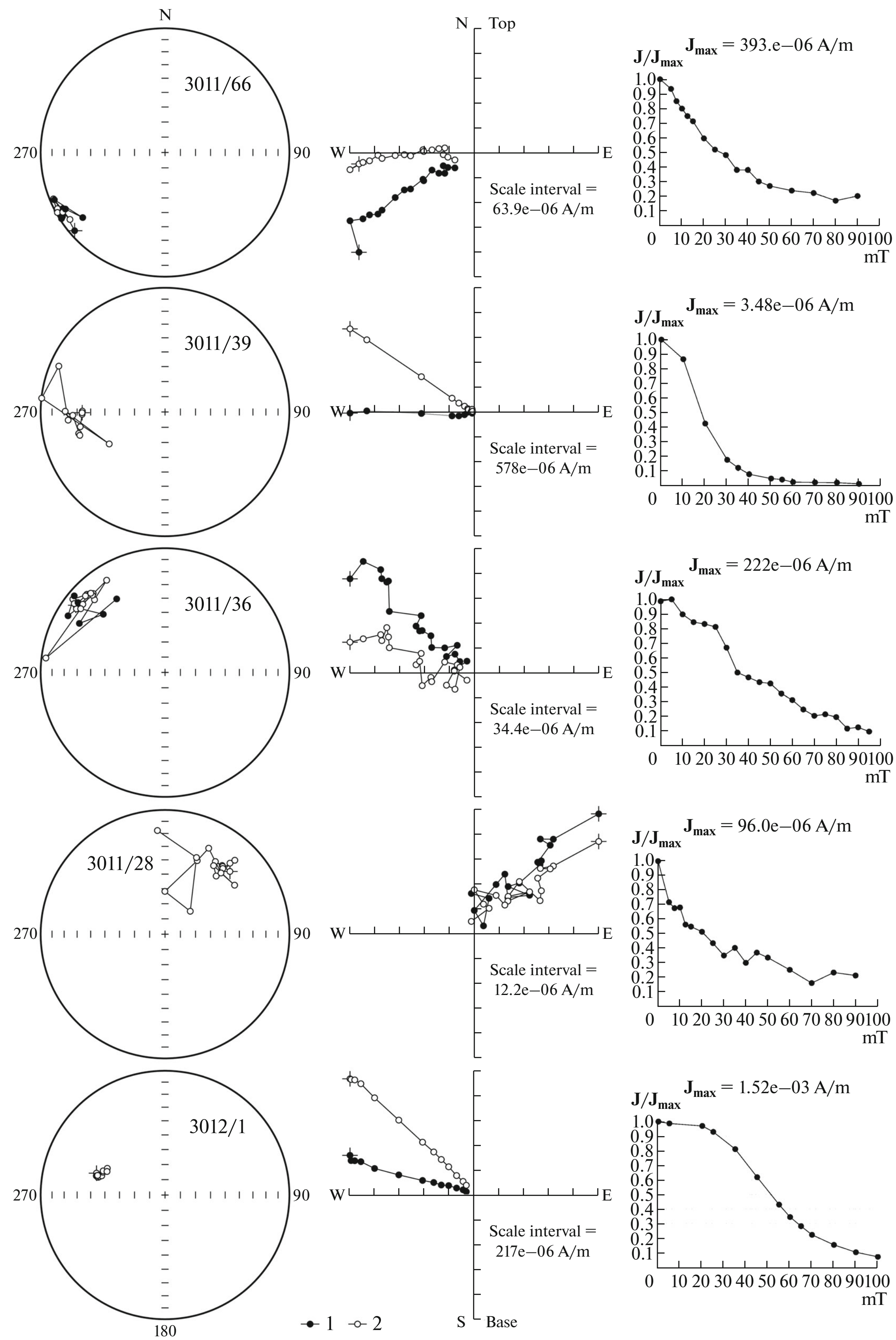

Fig. 9. Results of the component analysis (from left to right): stereographic illustrations of changes in vectors $\mathbf{J_n}$ during thermal cleaning sessions, Zijderveld diagrams (in the geographic coordinate system), and plots of sample demagnetization. (1, 2) $\mathbf{J_n}$ projections on the horizontal (1) and vertical (2) planes. For other symbols, see Fig. 8.

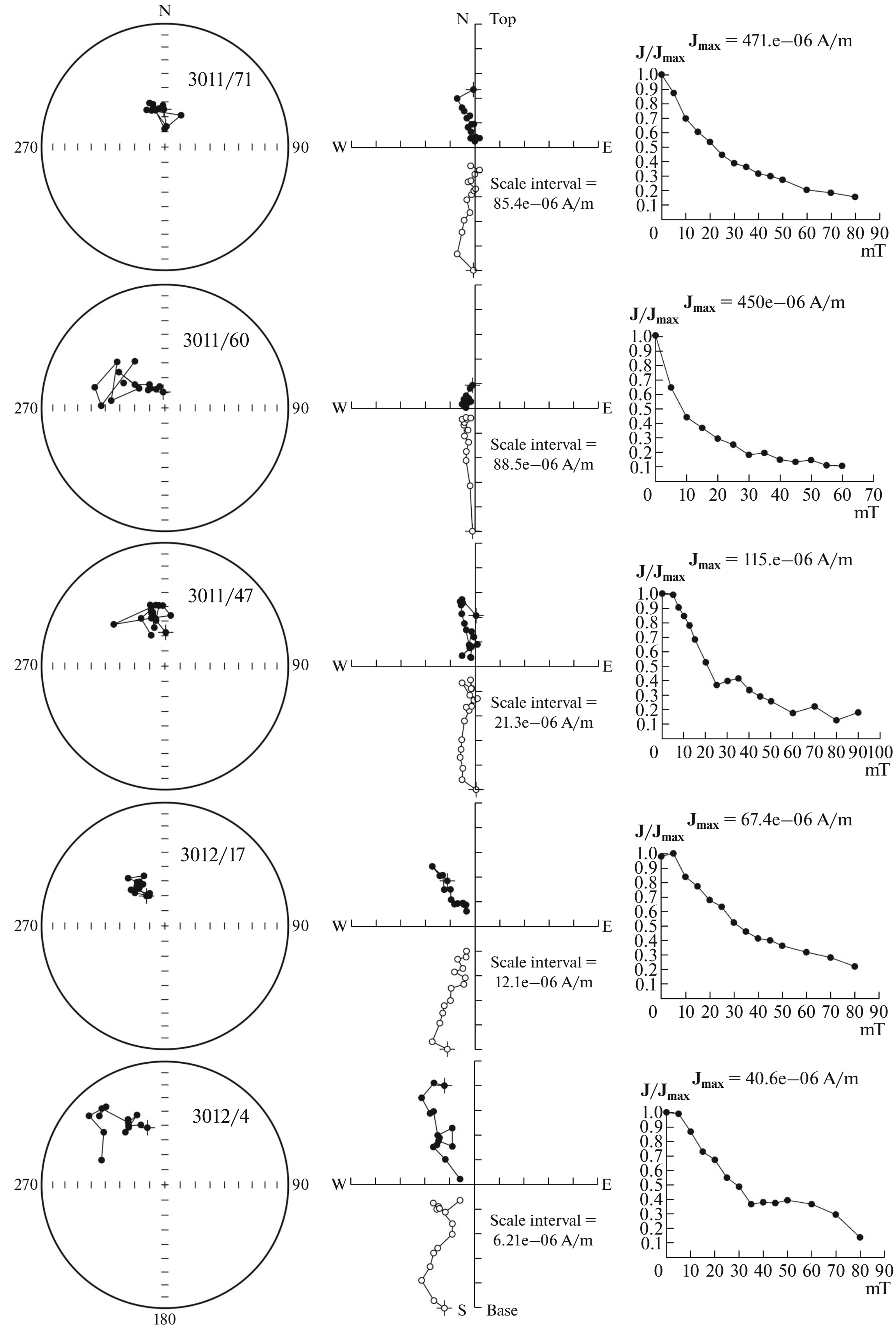
N
3011/71
270
90
N
Top
W
E
Scale interval = 85.4e–06 A/m
J/Jmax
Jmax = 471.e–06 A/m
mT
3011/60
Scale interval = 88.5e–06 A/m
Jmax = 450e–06 A/m
3011/47
Scale interval = 21.3e–06 A/m
Jmax = 115.e–06 A/m
3012/17
Scale interval = 12.1e–06 A/m
Jmax = 67.4e–06 A/m
3012/4
Scale interval = 6.21e–06 A/m
Jmax = 40.6e–06 A/m
180
S
Base

Fig. 9. (Contd.)

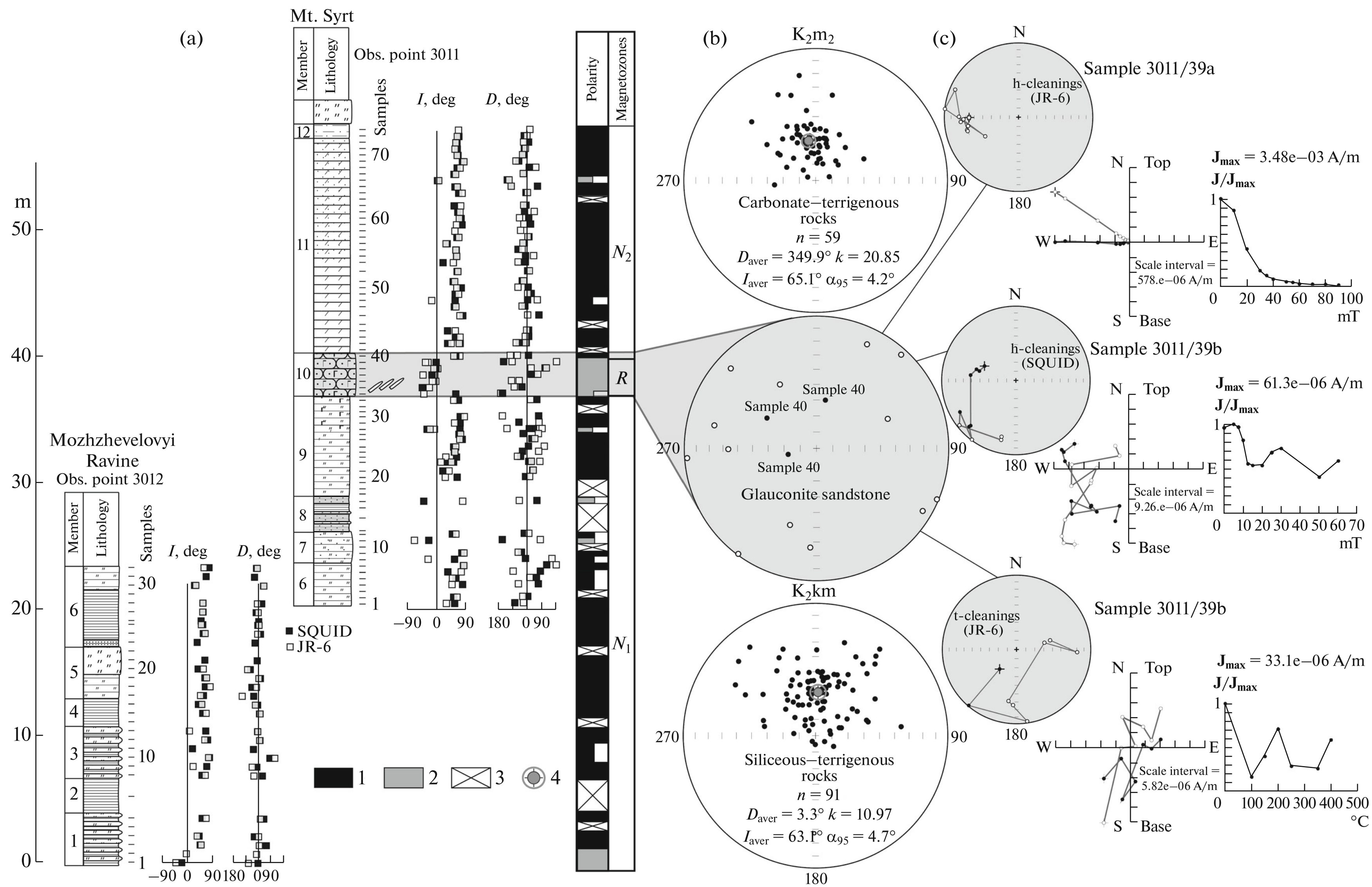

Fig. 10. Results of magnetostratigraphic investigations of the Nizhnyaya Bannovka section. (a) Plots of paleomagnetic declination (*D*) and inclination (*I*) and paleomagnetic record. Geomagnetic polarity: (1) normal, (2) reverse, (3) no data on polarity, (4) average paleomagnetic direction and confidence circle. (b) **ChRM** stereographic projection and paleomagnetic statistics for different rock lithotypes. (*n*) Number of samples in the selection; (D_{aver}, I_{aver}) average paleomagnetic declination and inclinations, respectively; (k) paleomagnetic precision parameter; (α_{95}) radius of 95% confidence circle. For legend, see Fig. 8. (c) Comparison of results of magnetic cleaning of glauconite sandstone samples on the JR-6 spinner magnetometer at Saratov University and 2G-Enterprices cryogenic magnetometer at IFZ (Moscow). For legend, see Fig. 8.

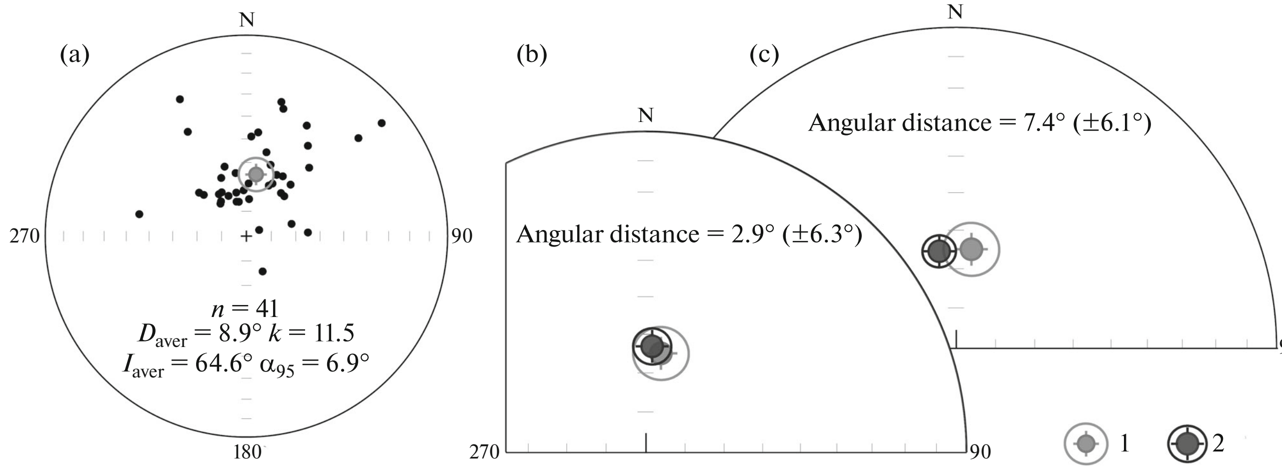

Fig. 11. Comparison of average paleomagnetic directions defined in the Campanian Vol'sk (1) and Campanian–Maastrichtian Nizhnyaya Bannovka (2) sections. (a) **ChRM** stereographic projection for the Campanian interval of the Vol'sk section (Guzhikova and Bagaeva, 2013); (b) average **ChRM** for the Campanian of the Vol'sk and Maastrichtian (Members 1–9) Nizhnyaya Bannovka sections; (c) average **ChRM** for the Campanian of the Vol'sk and Maastrichtian (Members 11–12) of Nizhnyaya Bannovka sections. Angular distances formed by average vectors are given with errors (±) determined by statistics of these vectors, according to (Debiche and Watson, 1995). If the angle exceeds the error, vectors demonstrate significant difference; in the opposite situation, vectors statistically correspond to each other. For legend, see Fig. 8.

tion allows a statement that the defined succession of magnetozones in the paleomagnetic record of the Nizhnyaya Bannovka section reflects variations in the geomagnetic field at the end of the Cretaceous Period. The obtained data are in accord with six of eight criteria accepted for the assessment of reliability of magnetostratigraphic conclusions (*Dopolneniya*..., 2000) and six (of seven possible) criteria proposed for the assessment of paleomagnetic data in (Van der Voo, 1993). This is sufficient for evaluating data on magnetic polarity obtained for the Nizhnyaya Bannovka section as being formally reliable.

DISCUSSION

Stratigraphy. The basal part of Member 10 contains the belemnite assemblage of the upper Campanian Belemnitella langei Zone; therefore, the lower boundary of the Maastrichtian Stage cannot be placed in the section below Sample 3011/37. This inference is to some extent consistent with the presence of the transitional Campanian–Maastrichtian radiolarian assemblage (Rhombastrum Beds, Sample 3011/32) in the uppermost part of Member 9 and late Maastrichtian calcareous dinocysts in the basal layers of Member 11 (Sample 3011/44). The finding of *Silicosigmoilina volganica* (Kuzn.), a characteristic species of the benthic foraminiferal assemblage from the LC19 Zone, is also in accordance with the conclusion on the late Campanian age of the uppermost part of Member 9 and Member 10 since, according to recent data, the lower boundary of the Maastrichtian Stage on the East European Platform is located inside the LC19 Zone (Guzhikov et al., 2014a, 2014b).

The data on benthic foraminifers (establishment of the Spiroplectammina kasanzevi and Anomalinoides pinguis beds) indicate unambiguously the late Maastrichtian age of Member 11 (Fig. 4). It should be noted that the A. pinguis Zone is defined in the upper Maastrichtian interval of Poland (Gawor-Biedowa, 1992) and the Caspian region (Naidin and Beniamovsky, 2006). The S. kasanzevi Zone in the Upper Cretaceous scale of West Siberia is correlated with the upper Maastrichtian (*Foraminifery*..., 1964; Marinov et al., 2014). Radiolarians (Plate IV) and calcareous dinocysts (Plate II) found in Member 11 (Fig. 5) substantiate its attribution to the upper Maastrichtian.

The lower part of the *R* zone confined to sediments with the belemnite assemblage of the B. langei Zone (Samples 3011/34–3011/37) may represent only an analog of Chron 32r since the latter represents only one large epoch of normal polarity in the late Campanian (Fig. 12). The higher part of Member 10 (Samples 3011/38 and 3011/39) located within the *R* zone corresponds probably also to Chron 32r, while the uppermost part of glauconite sand (Sample 3011/40) characterized by normal polarity is correlated with initial Chron 32n (or Subchron 32r.1n) At the same time, its belonging to Chron 31r cannot be ruled out, if a large hiatus is admitted in the uppermost part of Member 10. The N_2 magnetozone characterizing the carbonate–terrigenous sequence with upper Maastrichtian assemblages of benthic foraminifers (Members 11 and12) should correspond to late Maastrichtian Chron 31n or to the interval of late Maastrichtian chrons 31n and 30 (Fig. 12).

For coordination of all available data, it is necessary to admit the presence of a large hiatus corre-

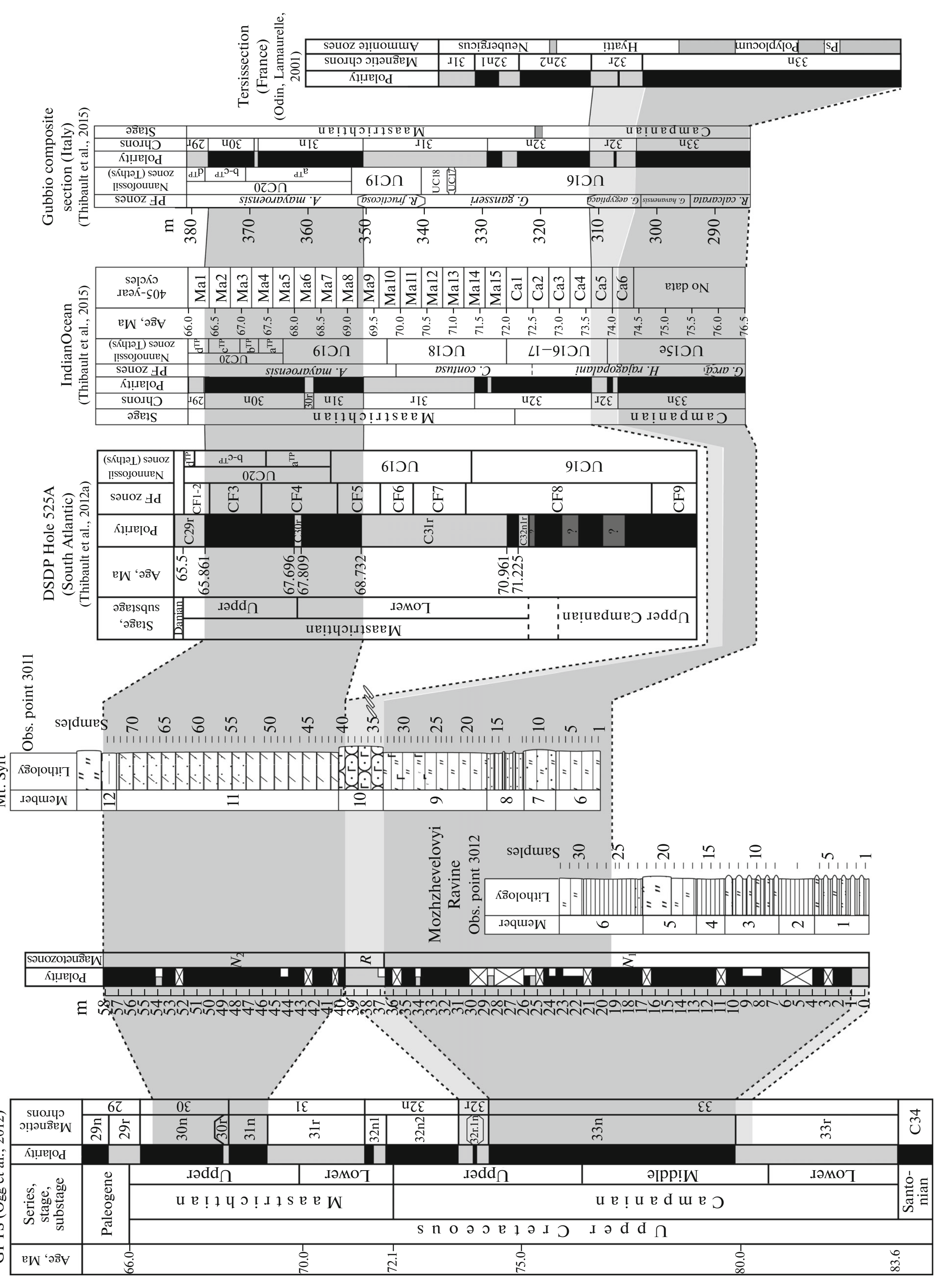

Fig. 12. Correlation of Campanian–Maastrichtian magnetostratigraphic sections of different regions with the geomagnetic polarity scale (GPTS). For legend, see Fig. 10.

sponding to the terminal Campanian (Belemnella licharewi Zone) and the lower Maastrichtian substage (Fig. 12). The correlation between the paleomagnetic record in the section under consideration and scale of magnetic polarity (GPTS) (Ogg et al., 2012) allows the duration of this lacune in sedimentation to be estimated as lasting at least 4.5 m.y. (Fig. 12). At first glance, the hiatus surface should be placed at the top of sandstone (Fig. 1). At the same time, the maximum $\mathbf{J_n}$ values at the level of Samples 3011/38 and 3011/39 (Figs. 6, 13) are most likely explained by the high concentration of extraterrestrial ferromagnetic minerals due to sharp deceleration of sedimentation rates. Therefore, it may be assumed that the hiatus corresponds to the level of Sample 3011/39, particularly taking into consideration the fact that precisely this level is marked by the replacement of reverse polarity by normal polarity (Fig. 1). In such a situation, the top of glauconite sand (Sample 3011/40) may correspond to the onset of a new transgressive cycle (Ogg et al., 2012). The Spongurus marcaense–Tholodiscus densus Beds in overlying carbonate clays (Samples 3011/43–3011/53) were likely formed still in depositional environments with decelerated sedimentation rates, which is evident from incrustation of radiolarian skeletons by calcareous nannofossils.

Thus, new bio- and magnetostratigraphic data changed the view on age of the terrigenous–carbonate sequence in the section under consideration (Fig. 3). Member 10 (probably, except for its uppermost part) is correlated with the upper Campanian B. langei Zone, while Member 11 belongs to the upper Maastrichtian substage (Fig. 12).

Nevertheless, it should be noted that the position of the boundary between the lower and upper Maastrichtian substages in GPTS cannot be considered as unambiguously established. It is based on the results of the paleomagnetic study of North American sections (Hicks et al., 1999), where the base of the upper Maastrichtian substage is correlated with the base of the ammonite Hoploscaphites birkelundi Zone (Hardenbol et al., 1998). The Zumaya reference section in northern Spain, where the base of the upper Maastrichtian substage is proposed to be placed at the first appearance level of the ammonite species *Pachydiscus fresvillensis* (Odin et al., 1996), unfortunately, has no paleomagnetic characteristics. In the paleontologically substantiated Gubbio (Italy) section, the uppermost part of Chron 31r (i.e., approximately correlative with the base of the upper Maastrichtian substage in Canada) corresponds to the base of the PF A. mayaroensis Zone and uppermost part of the nannofossil UC19 Zone (Fig. 12). At the same time, the nannofossil and foraminiferal units are diachronous at the global scale, which was confidently shown for the Maastrichtian in (Thibault et al., 2012a, 2015) by calibration of microfaunal succession in deep-sea holes drilled in the South Atlantic and Indian Ocean and sections of Europe (Fig. 12) using paleomagnetic and isotopic data. The difficulties related to the substantiation of the base of the upper Maastrichtian substage based on belemnites through the European paleobiogeographic region are discussed in (Kopaevch et al., 1987). Thus, the selection of criterion for tracing the base of the upper Maastrichtian substage by analogy with the potential type section of its boundary in Spain remains a topical problem. In our opinion, the problem may be solved if the base of Chron 31n is accepted, following (Ogg et al., 2012), as representing a primary reference level for the substage boundary. The advisability in using paleomagnetic features for substantiation of boundaries of general stratigraphic units was also noted in (Guzhikov and Baraboshkin, 2006; Guzhikov, 2013b).

The Prunobrachium mucronatum–Lithostrobus turitella Beds correspond to the particular stage in development of radiolarians, which demonstrate differences in their assemblages from both lower Campanian sediments and upper Campanian Prunobrachium articulatum Beds. This provides every reason for discussing the three-member subdivision of the Campanian Stage. In our opinion, the necessity for the subdivision of the longest (11 m.y.) Upper Cretaceous stage into three substages as is accepted in the standard stratigraphic scale (SSS) (Ogg et al., 2012), not into two substages as in the general stratigraphic scale (GSS) (*Stratigraficheskii*..., 2006), long ago became urgent. The discrepancy in the substage subdivision of the Campanian Stage in the GSS and SSS was denoted as one of the topical problems of the Cretaceous System in Russia (Baraboshkin et al., 2013). The idea of the three-member structure of the Campanian Stage is supported by best experts in the Cretaceous System of different regions (Petrizzo et al., 2011; Falzoni et al., 2013; *Stratigrafiya*..., 2013; Sel'tser and Beniamovsky, 2014). In the Russian special literature, the three-member subdivision of the Campanian Stage was first proposed for Cretaceous reference sections of Mangyshlak, where the Brotzenella monterelensis Zone (LC14) (Kopaevich et al., 1999) corresponding to the ammonite Haplitoplacenticeras coesfeldienses and belemnite Belemnitella mucronata mucronata zones was attributed to the middle Campanian substage (Olfer'ev and Alekseev, 2003, 2005; Olfer'ev et al., 2004). The base of the coesfeldiense Zone corresponds, in turn, to the lower boundary of the Haplitoplacenticeras marroti–H. vari Zone correlative with the middle Campanian boundary in Western Europe (Hardenbol et al., 1998).

Paleogeography. The transition between the Campanian and Maastrichtian ages was marked by the global sea level fall (Ogg et al., 2012) related to cooling in the terminal Campanian (Miller et al., 1999). The relatively long (up to 1.0–2.5 m.y.) episode of oceanic water cooling accompanied by the negative carbon isotope shift is proposed to be defined as the "Campanian–Maastrichtian boundary event" (CMB or CMBE) (Voigt et al., 2010, 2012). As is established, it was global, although it was differently expressed in different world basins (Jung et al., 2012; Niebuhr et al., 2011; Thibault et al., 2012a, 2012b). In the Nizhnyaya Bannovka section, the onset of the CMBE episode corresponds likely to the level of Sample 3011/28 in the uppermost part of Member 9 (Fig. 13) marked by glauconitization of opoka-like clays replaced higher in the section by glauconite sand of Member 10.

The remarkable feature of Late Cretaceous and Paleogene basins in the Saratov region was the intermittent formation of conditions favorable for development of various organisms with siliceous skeletons (Akhlestina et al., 2013; Oreshkina et al., 2013). Correspondingly, these basins accumulated large volumes of sediments variably enriched with SiO_2, which were subsequently transformed into various siliceous rocks. In the section under consideration, the stage of siliceous–clayey sedimentation is reflected in Members 1–9. The beginning of glauconitization in the uppermost part of Member 9 is marked by the radiolarian collapse, i.e., mass extinction of Campanian radiolarians dominated by characteristic species of the genus *Prunobrachium* (Fig. 13). Representatives of this genus populated relatively shallow cold-water (or with moderately cold water) basins near the shoreline (Amon, 2000). With respect to their paleobiogeography, they are typical boreal dwellers, which were widespread in the middle- and high-latitude basins of the Pechora, West Siberia, and Koryak–Kamchatka regions (Vishnevskaya, 2001).

Unlike radiolarians, benthic foraminifers are practically missing from siliceous Members 1–9. Single and rare representatives of their agglutinated species indicate unfavorable habitat conditions. According to Baryshnikova (1978), the extreme scarcity of benthic foraminiferal assemblages reflects the stagnant regime in the basin; in the opinion of other researchers (Naidin et al., 2008), it was characterized by almost anoxic conditions near the bottom or in the entire water column. Quite different aerobic conditions are reconstructed from diverse assemblages of benthic foraminifers from carbonate clays of Member 11, which are very similar, as was mentioned, to BF assemblages from the Gan'kino Formation of the Trans-Urals region and West Siberia. The late Campanian was marked by the opening of the Ayat seaway located in the Orsk graben between the Southern Urals and Mugodzhary (Amon, 2001). This stimulated ingression of water masses from the East European basin into the southern half of the West Siberian sea, where Santonian–Campanian siliceous–terrigenous sediments are replaced up the section by carbonate–terrigenous facies of the Maastrichtian Gan'kino Formation (Umova et al., 1968). The share of European foraminiferal species in North Turgai assemblages amounts to 50% (Amon, 1990; Beniamovskii and Kopaevich, 2002). Some of them colonized northerly areas in the West Siberian sea (Kissel'man, 1969). They include species characteristic of upper Campanian (*Bolivinoides decoratus*, *B. laevigatus*, *Heterostomella foveolata*, *Neoflabellina praereticulata*, *Bolivinoides draco miliaris*), upper Campanian–lower Maastrichtian (*Neoflabellina reticulata*), and lower Maastrichtian (*Falsoplanulina multipunctata*) sections in the European paleobiogeographic region. The assemblages from this part of the West Siberian sea are ecotonic since they include abundant endemic species dominated by agglutinated forms in addition to European immigrants. The northern part of the West Siberian sea remained under the influence of boreal waters from the Arctic basin, where microbiota was dominated by agglutinated foraminiferal and radiolarian species (*Foraminifery...*, 1964; Kissel'man, 1969; Beniamovskii and Kopaevich, 2002). The opposite process was also in progress: Transuralian species of benthic foraminifers such as *Anomalinoides globigeriniformis* and *A. pinguis* migrated to basins of the East European Platform. The distribution of these species in basins was diachronous: in the West Siberian paleobasin, they appear in the Campanian interval of the Gan'kino Formation (Marinov et al., 2014), while they migrated into the East European sea in the terminal early Maastrichtian (Beniamovsky et al., 2012, 2014). In the Poland basin, wide distribution of these species is noted for the late Maastrichtian (Gawor-Biedova, 1992). Unfortunately, magnetostratigraphic sections of the Gan'kino Formation (Lebedeva et al., 2013; Gnibidenko et al., 2014) have no microfaunal substantiation, which prevents controlling the diachronism/synchronism in the distribution of the species in question using paleomagnetic data.

The appearance of planktonic foraminifers, calcareous dinocysts, and diverse nannofossils in the lower part of Member 11 indicates that upper Maastrichtian carbonate clays were deposited during the warm transgression phase (Fig. 13). It is conceivable that this warm phase was related to the eustatic sea level rise during the global mid-Maastrichtian warming revealed by the study of surface water paleotemperatures in the Cretaceous sea of northwestern Europe (Thibault et al., 2016). The synchronism in these event is evident from paleomagnetic data: intervals corresponding to surface water warming in the Nizhnyaya Bannovka section are confined to Chron 31r as in sections of northwestern Europe (Thibault et al., 2016).

The peculiar feature of the upper Maastrichtian carbonate–terrigenous sequence is represented by distinct tendencies toward the growth of $\mathbf{J_n}$ and $\mathbf{J_{rs}}$ and simultaneous decrease in the $K/\mathbf{J_{rs}}$ parameter values (Fig. 6). These trends correspond to the increase in the share of the clayey component in clays noted during visual examination of the section and confirmed by the study of thin sections (five samples from Member 11). The growth of the $K/\mathbf{J_{rs}}$ values in this part of the section was a previously known phenomenon, which was related to the increase in concentrations of ferromagnetic particles in sediments during intensification of

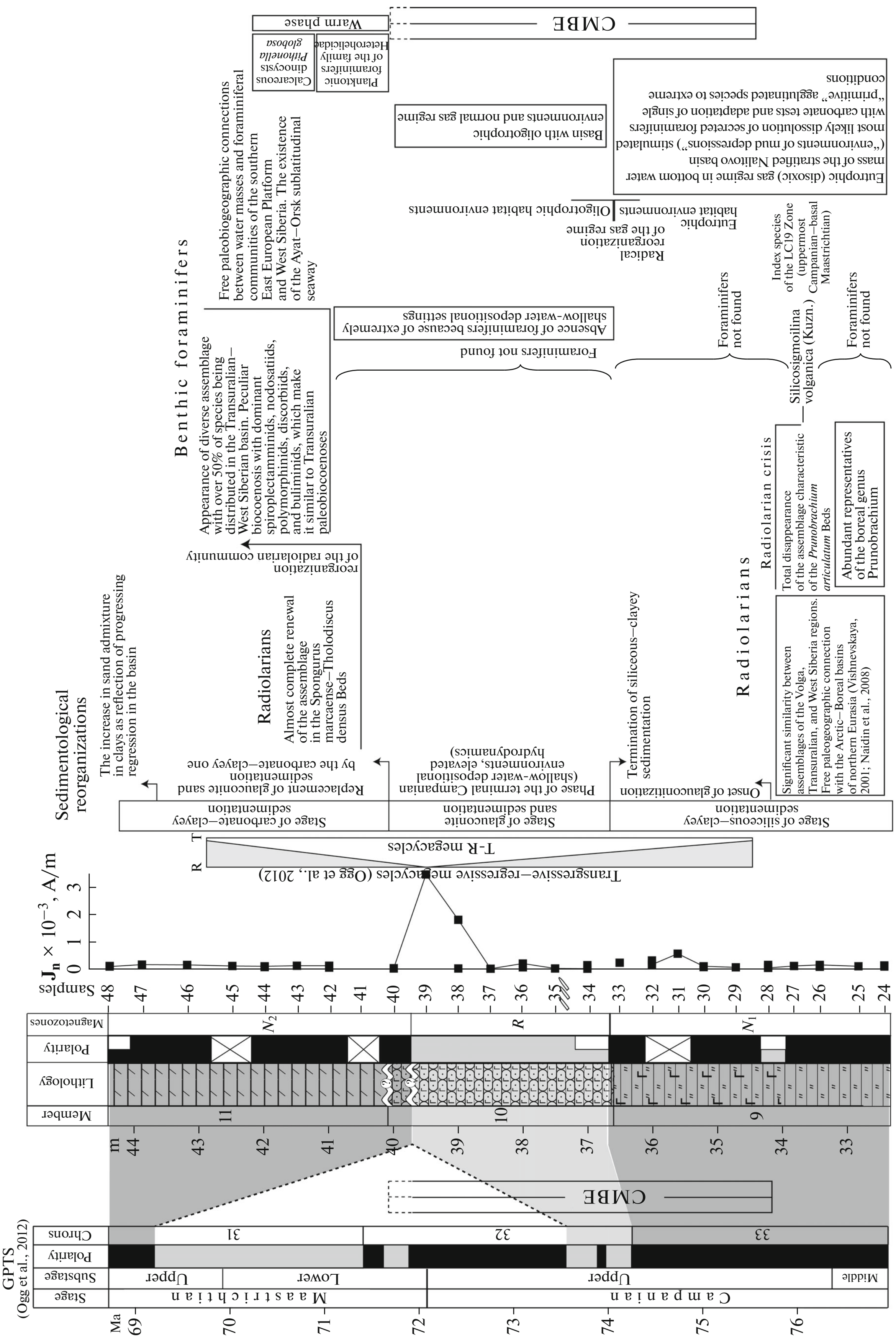

Fig. 13. The calendar of biotic and abiotic events in the terminal Campanian–Maastrichtian derived from the data on the Nizhnyaya Bannovka section. For legend, see Fig. 8.

the terrigenous influx (Abakshin et al, 1992; Fomin et al., 2006). Our paleomagnetic measurements on the high-sensitivity equipment revealed that the increase in $\mathbf{J_{rs}}$ is accompanied by the increase in $\mathbf{J_n}$, implying the decrease in average sizes of their particles, which leaves, however, the *K* values practically unchanged. Such a petromagnetic affinity excludes the role of silty–sandy detrital grains as carriers of magnetization (otherwise, the $\mathbf{J_n}$ value should decrease with simultaneous growth of the *K* value). At the same time, it is readily explainable by the upward increase in concentrations of extraterrestrial matter owing to intensified meteoric bombardment of the Earth in the Maastrichtian (Korchagin, 2013). The enrichment of sediments with submicron-sized ferromagnetic particles leaves the *K* value almost unchanged, but notably decreases $K/\mathbf{J_{rs}}$ and increases $\mathbf{J_n}$ owing to perfect orientation of the meteoric dust particles along the geomagnetic field. The microprobe investigations reveal abundant magnetite spherules and iron flakes (Fig. 7d) in the section, indirectly confirming our assumption.

CONCLUSIONS

The integrated investigations of the Campanian–Maastrichtian Nizhnyaya Bannovka section in the southern Saratov region on the Volga River right bank yielded the following results.

(1) The paleontological and biostratigraphic characteristics of the section are substantially improved.

First, it is established that sediments of this section contain belemnite species *Belemnitella pseudolanceolata* Jeletzky and *Belemnitella langei* Jeletzky, in addition to traditionally found *Belemnitella lanceolata* (Schloth.), which allowed host sediments to be attributed to the upper Campanian Belemnitella langei Zone.

The defined benthic foraminiferal assemblages indicate the presence of the Spiroplectammina kasanzevi and Anomalinoides pinguis beds in the section, which makes it possible to attribute the host sediments previously dated back to the early Maastrichtian to its upper substage.

The revealed radiolarian Prunobrachium mucronatum–Lithostrobus turitella Beds, which indicate the possibility of defining the middle Campanini on the East European Platform, serve as an additional argument in favor of subdivision of the Campanian Stage in the general stratigraphic scale into three substages (instead of two in Russia) by analogy with its three-members structure in the standard stratigraphic scale. It is established that the defined radiolarian P. articulatum Beds are widespread in upper Campanian sections of both the East European Platform and West Siberian plate (Vishnevskaya, 2009, 2010). The Rhombastrum Beds (transitional Campanian–Maastrichtian) and Spongurus marcaense–Tholodiscus densus Beds (upper Maastrichtian) are established for the first time.

The calcareous dinocyst Pithonella globosa Beds and nannofossil Discorhabdus ignotus–Prediscosphaera bukryii Assemblage are also first defined in the upper Maastrichtian interval.

(2) The first reliable magnetostratigraphic data obtained for the Niznyaya Bannovka section made it possible to establish magnetozones N_1, R, and N_2, analogs of magnetic chrons 33n, 32r, and 31n. It is assumed that magnetozone N_2 may correspond not only to Chron 31n but also to Chron 30.

(3) The bio- and magnetostratigraphic data imply the large sedimentation break during the Campanian–Maastrichtian transition lasting at least 4.5 m.y. and corresponding to the terminal Campanian and early Maastrichtian.

(4) It is proposed to use the base of magnetic Chron 31n for determining the lower boundary of the upper Maastrichtian substage.

(5) The Campanian–Maastrichtian boundary event and related sea level fall in response to global cooling are reflected in section lithology. The terminal part of the Campanian Stage is marked by glauconitization and replacement of opokas and siliceous clays by shallow-water glauconite sandstones. The onset of glauconitization of sediments in the uppermost part of the Nalitovo Formation corresponds to the crisis in development of radiolarians: disappearance of prunobrachiids and appearance of a new assemblage.

(6) The appearance of planktonic foraminifers, calcareous dinocysts, and diverse nannofossils in the basal part of the carbonate clay sequence reflects transgression of warm waters and corresponds, according to paleomagnetic data, to the eustatic sea level rise in response to global warming (Thibault et al., 2016). At the same time, noteworthy is the extreme scarcity and low taxonomic diversity of benthic foraminifers as compared even with other Maastrichtian sections of the Saratov region on the Volga River right bank.

(7) It is established that benthic foraminiferal assemblages from the section under consideration are similar to their coeval counterparts in the Gan'kino Formation of West Siberia, which indicates the existence of paleobiogeographic connections between foraminiferal communities of epicontinental seas of Eastern Europe and West Siberia in the late Maastrichtian.

(8) The petromagnetic structure of the upper Maastrichtian part of the section in question is best explained by the enrichment of sediments in extraterrestrial matter due to intensified meteoritic bombardment of the Earth at the end of the Cretaceous Period (Korchagin, 2013).

(9) It is clear that new data on the Nizhnyaya Bannovka section are of great significance for specifying the stratigraphic subdivision of the terminal Cretaceous System in the Ulyanovsk–Saratov Trough. One of the authors of this work (Beniamovsky) argues that Member 10 should be defined as a new lithostrati-

graphic unit (Belogorsk Formation), Member 11 should be attributed to the Nikolaevskoe Formation, and Member 12 should be attributed to the Karamysh Formation. Others (Guzikov and Pervushov) believe that such conclusions are premature. All the authors (except for Beniamovsky) are unanimous in the opinion that the problem of defining local stratigraphic units in the Campanian–Maastrichtian sections of the Middle Volga (Saratov) region requires a comprehensive discussion and a special article.

ACKNOWLEDGMENTS

We are grateful to V.A. Tsel'movich and A.Yu. Kurazhkovskii (Borok Geophysical Observatory, IFZ) for microprobe analysis of samples; R.A. Voinova (Faculty of Geology, Moscow State University) for the preliminary treatment of foraminifers and radiolarians; M.N. Ovechkina (Geological Survey of Israel (Jerusalem) and Paleontological Institute of the Russian Academy of Sciences) and M.A. Ustinova (Geological Institute, Russian Academy of Sciences) for identification of nannofossls; A.G. Manikin, V.A. Grishchenko, A.M. Surinskii, and A.M. Mikhailov (Saratov State University) for their help in the field study of the section and laboratory investigations; V.E. Pavlov, R.V. Veselovkii, and other scientists from the laboratory of the main geomagnetic field and petromagnetism (Institute of Physics of the Earth) for measurements on the cryogenic magnetometer; A.V. Kravtsov for his help in photographing microfossils on the scanning microscope; and Martin Košták (Carlow University) for consulting on belemnites.

This work was supported by the Russian Foundation for Basic Research (project nos. 12-05-00196-a, 13-05-00745-a, 15-05-04099-a, 15-05-04700-a, 16-05-00207-a, 16-05-00363-a, 16-35-00219-mol_a, 16-35-00339-mol_a), the Russian Humanitarian Science Foundation (project no. 15-37-10100), and the Ministry of Higher Education and Science of the Russian Federation (state contract nos. 1757 and 0135-2014-0070).

Reviewers A.Yu. Kazanskii and A.S. Alekseev

REFERENCES

Abakshin, O.V., Bogachkin, A.B., Guzhikov, A.Yu., and Fomin, V.A. The use of scalar magnetic parameters for stratigraphy and paleogeography, *Byull. RMSK po Tsentru i Yugu Russ. Platf.*, 1992, vol. 1, pp. 62–66.

Akhlestina, E.F., Ivanov, A.V., and Pervushov, E.M., The role of siliceous organisms in the sedimentation within Late Cretaceous and Paleogene deposits of the Volga Region, *Tr. NII Geol. SGU. Nov. Ser.*, 2001, vol. 7, pp. 19–30.

Aleksandrova, G.N., Beniamovsky, V.N., Vishnevskaya, V.S., and Zastrozhnov, A.S., New data on Upper Cretaceous biostratigraphy of the Lower Volga Region, *Stratigr. Geol. Correl.*, 2012, vol. 20, no. 5, pp. 426–465.

Alekseev, A.S., Kopaevich, L.F., Ovechkina, M.N., and Olferiev, A.G., Maastrichtian and Lower Paleocene of Northern Saratov Region (Russian Platform, Volga River): foraminifera and calcareous nannoplankton, *Bull. Inst. R. Sci. Nat. Belg., Sci. Terre*, 1999, vol. 69, pp. 15–45.

Amon, E.O., The Cretaceous–Paleogene boundary in the Middle and Southern Trans-Urals based on the stratigraphic distribution of microfaunistic assemblages, in *Problemy stratigrafii Urala. Mezozoi i kainozoi* (Problems in the Stratigraphy of the Urals: Mesozoic and Cenozoic), Sverdlovsk: Preprint, 1990, pp. 25–39.

Amon, E.O., Upper Cretaceous radiolarians of the Urals, in *Mater. Stratigr. Paleontol. Urala. Vyp. 5* (Data on Stratigraphy and Paleontology of the Urals), Yekaterinburg: Inst. Geol. Geochem. UBr RAS, 2000, no. 5, pp. 1–209.

Amon, E.O., Sea water areas of Urals in the Middle and Late Cretaceous, *Geol. Geofiz.*, 2001, vol. 43, no 3, pp. 471–483.

Arkhangelsky, A.D., Upper Cretaceous Deposits of the East European Russia, in *Materialy dlya geologii Rossii* (Data on the Geology of Russia), St. Petersburg: Tipogr. Imper. Akad. Nauk, 1912, vol. 25.

Arkhangelsky, A.D. and Dobrov, S.A., Essay on the geology of the Saratov Province, *Mater. po izucheniyu estestvenno-istoricheskikh uslovii Saratovskoi gubernii* (The Data on Studying the Natural–Historical Conditions in the Saratov Province), Moscow: Tov. "Pechatnya S.P. Yakovleva," 1913, vol. 1.

Baraboshkin, E.Yu., Arkadiev, V.V., Beniamovsky, V.N., et al., The Cretaceous stratigraphic scale of Russia: current state, main problems, ways of perfection, in *Mater. Vseross. konf. "Obshchaya stratigraficheskaya shkala Rossii: sostoyanie i perspektivy obustroistva"*, Moskva, 23–25 maya 2013 g. (Proc. All-Russ. Conf. "General Stratigraphic Scale of Russia: Current State and Ways of Perfection), Fedonkin, M.A., Ed., Moscow: Geol. Inst. Russ. Akad. Nauk, 2013, pp. 289–297.

Baryshnikova, V.I., Ivanova, A.N., Morozov, N.S., and Khabarova, T.N., Upper Cretaceous stratigraphy of the Saratov and Stalingrad Volga regions, in *Tr. Vsesoyuz. soveshch. po utochneniyu unifitsirovannoi skhemy stratigrafii Mezozoiskikh otlozhenii Russkoi platformy. Tr. VNIGNI* (Proc. All-Russ. Petrol. Explor. Inst.), 1961, Iss. XXIX, vol. 3, pp. 110–119.

Baryshnikova, V.I., Age and formation environment of siliceous clays below the Lanceolate Level, the Volga right side near Saratov, in *Vopr. stratigrafii i paleontologii* (Problems in Stratigraphy and Paleontology), Saratov: Saratov. Gos. Univ., 1978, no. 3, pp. 81–89.

Beniamovsky, V.N., Late Cretaceous–Early Paleogene paleogeographic scenarios within the northern periphery of the Tethys, in *Biosfera-ekosistema-biota v proshlom Zemli (paleobiogeograficheskie aspekty).Tr. GIN RAN* (Biosphere–Ecosystem–Biota in the Past of the Earth (Paleobiogeographical Aspects). Proc. Geol. Inst. Rus. Acad. Sci.), 2005, vol. 516, pp. 267–308.

Beniamovsky, V.N., Alekseev, A.S., Ovechkina, M.N. et al., Upper Campanian–Lower Maastrichtian sections of the northwestern Rostov region. Article 1. Description, paleontological assemblages, and lithobiostratigraphy, *Stratigr. Geol. Correl.*, 2012, vol. 20, no. 4, pp. 346–379.

Beniamovsky, V.N., Alekseev, A.S., Podgaetskii, A.V., et al., Upper Campanian–Lower Maastrichtian sections of Northern Rostov Oblast: Article 2. Depositional environments and paleogeography, *Stratigr. Geol. Correl.*, 2014, vol. 22, no. 5, pp. 518–537.

Beniamovsky, V.N. and Kopaevich, L.F., Late Santonian–Maastrichtian paleobiogeography of the Peri-Tethyan Basins of Europe, in *Tethyan/Boreal Cretaceous Correlation*, Michalik J., Ed., Bratislava: VEDA Publ. House Slovak Acad. Sci., 2002, pp. 173–185.

Bondareva, M.V., Morozov, N.S., and Bondarenko, N.A., Santonian, Campanian, and Maastrichtian deposits in the interfluve between Medveditsa and Volga rivers (the Volgograd right bank), in *Voprosy geologii Yuzhnogo Urala i Povolzh'ya* (Problems in Geology of the Southern Urals and Volga Region), 1981, vol. 22, pp. 84–94

Bondarenko, N.A., On the distribution of the Zone Belemnella licharewi in the Saratov Volga Region, in *Voprosy stratigrafii i paleontologii* (Problems in Stratigraphy and Paleontology), Saratov: Saratov. Gos. Univ., 1978, vol. 3, pp. 35–51.

Bondarenko, N.A., Stratigraphy and conditions of sedimentation of Santonian, Campanian and Maastrichtian stages of the right side of Lower Volga River basin, *Extended Abstract of Cand. Sci. Dissertation*, Saratov: Saratov. Gos. Univ., 1990.

Christensen, W.K., Upper Cretaceous belemnites from the Vomb Trough in Scania, Sweden, *Sver. Geol. Unders. Ser. C*, 1986, no. 57.

Christensen, W.K., Upper Cretaceous belemnite stratigraphy of Europe, *Cretaceous Res.*, 1990, vol. 11, no. 4, pp. 371–386.

Christensen, W.K., Upper Cretaceous belemnitellids from the Bastad Basin, Southern Sweden, *Geol. Foeren. Stockholm Foerh.*, 1993, vol. 115, pp. 39–57.

Christensen, W.K., Belemnitella from the Upper Campanian and Lower Maastrichtian chalk of Norfolk, England, *Spec. Pap. Palaeontol.*, 1995, no. 51.

Christensen, W.K., Upper Campanian and Lower Maastrichtian belemnites from the Mons Basin, Belgium, *Bull. Inst. R. Sci. Nat. Belg., Sci. Terre*, 1999, vol. 69, pp. 97–131.

Debiche, M.G. and Watson, G.S., Confidence limits and bias correction for estimating angles between directions with applications to paleomagnetism, *J. Geophys. Res.*, 1995, vol. 100, no. B12, pp. 24405–24430.

Dopolneniya k Ctratigraficheskomu kodeksu Rossii (Supplements to the Stratigraphic Code of Russia), St. Petersburg: Vseross. Nauchno-Issled. Geol. Inst., 2000 [in Russian].

Eremeeva, A.I. and Belousova, N.A., Foraminiferal stratigraphy of Cretaceous and Paleogene deposits of the eastern slope of the Urals, Trans-Urals, and North Kazakhstan, in *Mater. po geologii i poleznym iskopaemym Urala* (Data on Geology and Mineral Resources of the Urals),1961. vol. 9.

Falzoni, F. and Petrizzo, M.R., MacLeod, K.G., and Huber, B.T., Marine Santonian–Campanian planktonic foraminifera from Tanzania, Shatsky Rise, and Exmouth Plateau: species depth ecology and paleoceanographic inferences, *Micropaleontology*, 2013, vol. 103, pp. 15–29.

Fomin, V.A., Goncharenko, O.P., Zhukov, A.N., et al., Petromagnetic and mineralogical characteristics of the section of Cretaceous deposits (Pudovkino village, Saratov district), in *Nedra Povolzh'ya Prikaspiya* (Mineral Resources of the Saratov Volga Region and Caspian Sea Basin), 2006, vol. 47, pp. 37–45.

Foraminifers from Cretaceous and Paleogene Deposits of the West Siberian Lowland, in *Tr. VNIGRI* (Proc. All-Russ. Petrol. Res. Explor. Inst.), Subbotin, N.N., Ed., 1964, vol. 234.

Fütterer, D.K., Pithonelloid calcareous dinoflagellates from the Upper Cretaceous and Cenozoic of the southeastern Atlantic Ocean, DSDP Leg 74, *Ocean Drill. Program, Proc.: Initial Rep.*, 1984, vol. 74, pp. 533–541.

Gabdullin, R.R., *Ritmichnost' verkhnemelovykh otlozhenii Russkoi plity, Severo-Zapadnogo Kavkaza i Yugo-Zapadnogo Kryma (stroenie, klassifikatsiya, modeli formirovaniya)* (Rhythmicity of the Upper Cretaceous Deposits of the Russian Plate, North-Western Caucasus and South-Western Crimea (Composition, Classification, Models of Origin)), Moscow: Mosk. Gos. Univ., 2002 [in Russian].

Gawor-Beidova, E., Campanian and Maastrichtian foraminifera from the Lublin Upland, Eastern Poland, *Palaeontol. Pol.*, 1992, no. 52.

Gerasimov, P.A., Migacheva, E.E., Naidin, D.P., and Sterlin, B.P., Jurassic and Cretaceous deposits of the Russian Platform, in *Ocherki regional'noi geologii SSSR* (Essays on Regional Geology of the USSR), Moscow: Mosk. Gos. Univ., 1962, no. 5.

Glazunova, A.E., *Paleontologicheskoe obosnovanie stratigraficheskogo raschleneniya melovykh otlozhenii Povolzh'ya. Verkhnii mel* (Paleontological Substantiation ofthe Stratigraphical Subdivisions of the Cretaceous Sediments in the Volga River Region: Lower Cretaceous), Moscow: Nedra, 1972 [in Russian].

Gnibidenko, Z.N., Lebedeva, N.K., and Shurygin, B.N., A regional Upper Cretaceous magnetostratigraphic section of southern West Siberia (Omsk depression), *Dokl. Earth Sci.*, 2014, vol. 458, no. 1, pp. 1107–1111.

Grishanov, A.N., Paleomagnetic Section of Cretaceous Deposits of the Saratov Right Bank, in *Voprosy geologii Yuzhnogo Urala i Povolzh'ya. Stratigraficheskie i litologicheskie issledovaniya* (Problems in Geology of the Southern Urals and Volga Region: Stratigraphical and Lithologic Investigations), Saratov: Saratov. Gos. Univ., 1984, pp. 56–62.

Guzhikov, A.Yu. and Baraboshkin, E.Yu., Assessment of diachronism of biostratigraphic boundaries by magnetochronological calibration of zonal scales for the Lower Cretaceous of the Tethyan and Boreal belts, *Dokl. Earth Sci.*, 2006, vol. 409, no. 2, pp. 843–846.

Guzhikov, A.Yu., Solving unsolvable problems in stratigraphy (Comments to the paper "New data on the magnetostratigraphy of the Jurassic–Cretaceous boundary interval, Nordvik Peninsula (northern East Siberia)" by V.Yu. Bragin, O.S. Dzyuba, A.Yu. Kazansky, and B.N. Shurygin), *Russ. Geol. Geophys.*, 2013a. vol. 54, no. 3, pp. 349–354.

Guzhikov, A.Yu., Role of paleomagnetic criteria in justification of unit boundaries in the General Stratigraphic Scale of Russia, in *Mater. Vseross. Soveshch. "Obshchaya stratigraficheskaya shkala Rossii: sostoyanie i perspektivy obustroistva." Moskva, 23-25 maya 2013 g.* (Proc. All-Russ. Conf. "General Stratigraphic Scale of Russia: Current State and Ways of Perfection), Fedonkin, M.A., Ed., Moscow: Geol. Inst., 2013b, pp. 25–28.

Guzhikov, A.Yu., Baraboshkin, E.Yu., Beniamovsky, V.N., et al., Preliminary bio- i magnetostratigraphic data on the Campanian and Maastrichtian of the Aktulagai plateau (Kazakhstan), in *Melovaya sistema Rossii i blizhnego zarubezh'ya: problemy stratigrafii i paleogeografii* (Cretaceous System of Russia and CIS Countries: Problems of Stratigraphy and Paleogeography), Baraboshkin, E.Yu., Markevich, V.S., and Bugdaeva, E.V., , Eds., Vladivostok: Dal'nauka, 2014a, pp. 107–110.

Guzhikov, A.Yu., Beniamovsky, V.N., Baraboshkin, E.Yu., et al., On the Maastrichtian lower boundary in the Saratov Volga Region, in *Melovaya sistema Rossii i blizhnego zarubezh'ya: problemy stratigrafii i paleogeografii* (Cretaceous System of Russia and CIS Countries: Problems of Stratigraphy and Paleogeography), Baraboshkin, E.Yu., Markevich, V.S., Bugdaeva, E.V., Eds., Vladivostok, Dal'nauka, 2014b, pp. 103–106.

Guzhikova, A.A. and Bagaeva, M.I., New magnetostratigraphic data on the Campanian of the Saratov Volga right bank, in *Mater. Mezhd. shkoly-seminara "Problemy paleomagnetizma i magnetizma gornykh porod"* (Proc. Int. School-Seminar "*Problems in Paleomagnetism and Magnetism of Rocks*"), Kazan: Kazan. Gos. Univ., 2013, pp. 71–76.

Hardenbol, J., Thierry, J., Farley, M.B., et al., Mesozoic and Cenozoic sequence chronostratigraphic framework of European Basins, in *Mesozoic–Cenozoic Sequence Stratigraphy of European Basins*, De Graciansky P.-C. et al., Eds., *Spec. Publ.—SEPM (Soc. Sediment. Geol.),* 1998, vol. 60, pp. 763–781.

Hicks, J.F., Obradovich, J.D., and Tauxe, L., Magnetostratigraphy, isotopic age calibration and intercontinental correlation of the Red Bird Section of the Pierre Shale, Niobrara County, Wyoming, USA, *Cretaceous Res.*, 1999, vol. 20, pp. 1–27.

Jeletzky, J.A., Zur kenntnis der oberkreide der Dnjepr–Donetz–Senke und zum vergleich der russischen borealen Oberkreide mit derjenigen Polens und Nordwesteuropas, *Geol. för. Stockholm. Förh.,* 1948, vol. 70, no. 4, pp. 583–602.

Jung, C., Voigt, S., and Friedrich, O., High-resolution carbon-isotope stratigraphy across the Campanian–Maastrichtian boundary at Shatsky Rise (Tropical Pacific), *Cretaceous Res.*, 2012, vol. 37, pp. 177–185.

Kazintsova, L.I., Radiolarians from Upper Cretaceous Sediments of the Saratov Volga Region, in *Nedra Povolzh'ya Prikaspiya* (Mineral Resources of the Saratov Volga Region and Caspian Sea Basin), 2000, vol. 23, pp. 37–41.

Kiselman, E.N., Foraminifer-based subdivision of Upper Cenonian deposits of the West Siberian Lowland (Uppermost Campanian, Maastrichtian), in *Tr. SNIIGGiMS "Mater. po stratigrafii i paleontologii Sibiri"* (Proc. Siberian Res. Inst. Geol., Geophys. Min. Resour. "Data on Stratigraphy and Paleontology of Siberia"), 1969, vol. 8, pp. 163–175.

Kopaevich, L.F., Beniamovsky, V.N., and Naidin, D.P., Lower–Upper Maastrictian boundary in the European Paleobiogeographic Region, *Bull. Mosk O-va Ispyt. Prir., Ser. Geol.*, 1987, vol. 62, no. 5, pp. 43–57.

Kopaevich, L.F., Alekseev, A.S., Baraboshkin, E.Yu., and Beniamovsky, V.N., Cretaceous sedimentary units of Mangyshlak Peninsula (Western Kazakhstan), *Geodiversitas*, 1999, vol. 21, no. 3, pp. 407–418.

Kopaevich, L.F., Late Cretaceous planktonic foraminifers of East European Platform and its southern framing: zonal biostratigraphy, changes at main boundaries, paleoocenological reconstructions, *Extended Abstract of Doctoral (Geol.-Mineral.) Dissertation*, Moscow, 2011.

Korchagin, O.A., Fossil micrometeorites, microtektites and microkristites: method of investigations, classification and impact-stratigraphy scale, in *Stratigrafiya v nachale XXI veka—tendentsii i novye idei. Ocherki po regional'noi geologii Rossii* (Stratigraphy in the Beginning of the XXI Century—Trends and New Ideas. Notes on Regional Geology of Russia), Moscow: Geolkart-Geos, 2013, vol. 6, pp. 112–142.

Lagroix, F. and Banerjee, S.K., Cryptic post-depositional reworking in aeolian sediments revealed by the anisotropy of magnetic susceptibility, *Earth Planet. Sci. Lett.*, 2004, vol. 224, pp. 453–459.

Lebedeva, N.K., Aleksandrova, G.N., Shurygin, B.N., et al., Paleontological and magnetostratigraphic data on Upper Cretaceous deposits from borehole no. 8 (Russkaya Polyana District, Southwestern Siberia), *Stratigr. Geol. Correl.*, 2013, vol. 21, no. 1, pp. 48–78.

Lurcock, P.C. and Wilson, G.S., The palaeomagnetism of glauconitic sediments, *Global Planet. Change*, 2013, vol. 110, pp. 278–288.

Marinov, V.A., Sobolev, E.S., and Glinskikh, L.A., Foraminifera, ostracods, and ammonites in Upper Cretaceous deposits of the Gankino Formation (West Siberia): biostratigraphy, paleoecological reconstructions, and geographic links, *Litosfera*. 2014, no. 4, pp. 50–65.

Milanovskii, E.V., *Ocherk geologii Srednego i Nizhnego Povolzh'ya* (Essay on Geology of Middle and Lower Volga River), Moscow-Leningrad: Gostoptekhizdat, 1940 [in Russian].

Miller, K.G., Barrera, E., Olsson, R.K., et al., Does ice drive Early Maastrichtian eustacy?, *Geology*, 1999, vol. 27, pp. 783–786.

Molostovskii, E.A. and Khramov, A.N., *Magnitostratigrafiya i ee znachenie v geologii* (Magnetostratigraphy and Its Significance for Geology)*, Saratov*: Saratov. Gos. Univ., 1997 [in Russian].

Naidin, D.P., Subclass Endocochlia, Endocochleate Cehalopods, in *Atlas verkhnemelovoi fauny Severnogo Kavkaza i Kryma* (Atlas of Upper Cretaceous Fauna of North Caucasus and Crimea), Moscow: Gostoptekhizdat, 1959, pp. 198–209.

Naidin, D.P., Upper Cretaceous deposits of the Russian Platform, in *Tr. Vsesoyuz. soveshch. po utochneniyu unifitsirovannoi skhemy stratigrafii mezozoiskikh otlozhenii Russkoi platformy. Melovaya sistema i materialy kollokviuma po mikrofaune yurskikh i melovykh otlozhenii* (Proc. All-Union Conf. on the Improvements of the Unified Stratigraphic Scheme of the Mesozoic Sediments of the Russian Platform. Cretaceous System and Materials of the Workshop on the Microfauna of the Jurassic and Cretaceous Sediments), Leningrad: Gostoptekhizdat, 1961, vol. 3, pp. 75–80.

Naidin, D.P., Astronomic variations, climatic fluctuations, and rhythmicity of carbonate sequences: Communication 2. Climatic fluctuation and rhythmicity of Mesozoic Carbonate sequences, *Izv. Vuzov. Geol. Razved.*, 1990, no. 6, pp. 29–43.

Naidin, D.P. and Beniamovsky, V.N., The Campanian–Maastrichtian stage boundary in the Aktulagai Section (North Caspian Depression), *Stratigr. Geol. Correl.* 2006, vol. 14, no. 4, pp. 433–443.

Naidin D.P., Beniamovsky, V.N., Olfer'ev, A.G., et al., Demineralization in the epicontinental sea of the East European Platform. Part 1: Late Campanian demineralization of the Ulyanovsk–Saratov part of the sea, *Bull. Mosk O-va Ispyt. Prir., Ser. Geol.*, 2008, vol. 83, vol. 1, pp. 60–71.

Netskaya, A.I., Foraminifera of Upper Senonian deposits of Western Siberia, in *Tr. VNIGRI, Nov. ser.* (Proc. All-Russ. Petrol. Res. Explor. Inst. New. Ser.), 1948, vol. 31, pp. 211–225.

Niebuhr, B., Hampton, M.J., Gallagher, L.T., and Remin, Z., Integrated stratigraphy of the Kronsmoor section (northern Germany), a reference point for the base of the Maastrichtian in the Boreal Realm, *Acta Geol. Polon.*, 2011, vol. 61, no. 2, pp. 193–214.

Odin, G.S., Hancock, J.M., Antonescu, E., et al., Definition of a global boundary stratotype section and point for the Campanian/Maastrichtian boundary, *Bull. Inst. R. Sci. Nat. Belg., Sci. Terre*, 1996, vol. 66 (Suppl.), pp. 111–117.

Odin, G.S. and Lamaurelle, M.A., The global Campanian–Maastrichtian stage boundary, *Episodes*, 2001, vol. 24, no. 4, pp. 229–238.

Ogg, J.G., Hinnov, L.A., and Huang, C., Cretaceous, in *The Geologic Time Scale 2012*, Gradstein, F., Eds., Amsterdam: Elsevier, 2012.

Olfer'ev, A.G. and Alekseev, A.S., Biostratigraphic zonation of the Upper Cretaceous in the East European Platform, *Stratigr. Geol. Correl.*, 2003, vol. 11, no. 2. pp. 172–198.

Olfer'ev, A.G., Alekseev, A.S., Beniamovsky, V.N., et al., The Mezino–Lapshinovka reference section of the Upper Cretaceous and problems of Santonian–Campanian boundary in Saratov Area near the Volga River, *Stratigr. Geol. Correl.*, 2004, vol. 12, no. 6, pp. 603–636.

Olfer'ev, A.G. and Alekseev, A.S., *Stratigraficheskaya skhema verkhnemelovykh otlozhenii Vostochno-Evropeiskoi platformy. Ob"yasnitel'naya zapiska* (Stratigraphic Chart of the Upper Cretaceous Deposits of the East European Platform. Explanatory Note), Moscow: Paleontol. Inst. Ross. Akad. Nauk, 2005 [in Russian].

Olfer'ev, A.G., Beniamovsky, V.N., Vishnevskaya,V.S., et al., Upper Cretaceous deposits in the northwest of Saratov Oblast. Part 1: litho-and biostratigraphic analysis of the Vishnevoe Section, *Stratigr. Geol. Correl.*, 2007, vol. 15, no. 6, pp. 610–655.

Olfer'ev, A.G., Beniamovsky V.N., Vishnevskaya, V.S., et al., Upper Cretaceous deposits in the northwest of Saratov region, Part 2: Problems of chronostratigraphy and regional geological history, *Stratigr. Geol. Correl.*, 2008, vol. 16, no. 3, pp. 267–294.

Olfer'ev, A.G., Beniamovsky, V.N., Ivanov, A.V., et al., Upper Cretaceous deposits in the north of the Saratov Region. Part 1: the Bol'shevik Quarry section in the environs of the town of Vol'sk, *Bull. Mosk O-va Ispyt. Prir., Ser. Geol.*, 2009a, vol. 84, no. 2, pp. 5–22.

Olfer'ev, A.G., Beniamovsky, V.N., Ivanov, A.V., et al., Upper Cretaceous deposits in the northwest of Saratov Region. Part 2: biostratigraphic subdivision of the Bol'shevik Quarry section in the environs of the town of Vol'sk, *Bull. Mosk O-va Ispyt. Prir., Ser. Geol.*, 2009b, vol. 84, no. 4, pp. 29–46.

Olfer'ev, A.G., Sel'tser, V.B., Alekseev, A.S., et al., Upper Cretaceous deposits of the northern part of the Saratov Region. Part 3: biostratigraphic subdivision of the "Krasnyi Oktyabr" Quarry in the southern environs of the town of Vol'sk, *Bull. Mosk O-va Ispyt. Prir., Ser. Geol.*, 2014, vol. 89, no. 6. pp. 45–76.

Oreshkina, T.V., Lygina, E.A., Vozhzhova, O.A., and Ivanov, A.V., Diatoms and silicoflagellates of the Upper Cretaceous from Saratov Region: Biostratigraphy and sedimentation settings, *Stratigr. Geol. Correl.*, 2013, vol. 21, no. 2, pp. 222–236.

Ovechkina, M.N. and Alekseev, A.S., Changes in phyto- and zooplankton communities of the Maastrichtian Basin, Saratov Region near the Volga River, in *Ekosistemnye perestroiki i evolyutsiya biosfery* (Ecosystem Turnovers and Biosphere Evolution), Moscow: Paleontol. Inst. Ross. Akad. Nauk, 2004, vol. 6, pp. 57–73.

Ovechkina, M.N., *Izvestkovyi nannoplankton verkhnego mela (kampan i maastrikht) yuga i vostoka Russkoi plity* (Upper Cretaceous (Campanian and Maastrichtian)Calcareous Nannoplankton in the Southern and Eastern Parts of the Russian Plate), Moscow: Nauka, 2007 [in Russian].

Pechersky, D.M., Nurgaliev, D.K., Fomin, V.A., et al., Extraterrestrial iron in the Cretaceous-Danian sediments, *Izv., Phys. Solid Earth*, 2011, vol. 47, no. 5, pp. 379–401.

Pechersky, D.M., Naidin, D.P., and Molostovsky, E.A., The Santonian–Campanian reversed polarity magnetozone and the Late Cretaceous magnetostaratigraphical time-scale, *Cretaceous Res.*, 1983, vol. 4, pp. 251–257.

Pervushov, E.M., Arkhangelskii, M.S., and Ivanov, A.V., *Catalog mestonakhozhdenii ostatkov morskikh reptilii v yurskikh i melovykh otlozheniyakh Nizhnego Povolzh'ya* (Catalogue of Localities of Jurassic and Cretaceous Marine Reptiles in the Lower Volga Region), Saratov: GosUNTs "Kolledzh" 1999a [in Russian].

Pervushov, E.M., Ivanov, A.V., and Popov, E.V., Local stratigraphic scheme of the Upper Cretaceous deposits of the Volga River Basin (the right bank), in *Tr. NIIgeologii SGU. Nov. Ser.* (Proc. Res. Geol. Inst. Saratov State Univ. New. Ser.),1999b, vol. 1, pp. 85–94.

Pervushov, E.M., Sel'tser, V.B., Beniamovsky, V.N., et al., Biostratigraphic subdivision of Kokurino Section (Saratov region) and some aspects of Campanian stratigraphy in the Middle Volga Region, *Bull. Mosk O-va Ispyt. Prir., Ser. Geol.*, 2015, vol. 90, no. 2, pp. 51–84.

Pessagno, E.A., Radiolarian zonation and biostratigraphy of the Upper Cretaceous portion of the Great Valley Sequence, California Coast Ranges, *Micropaleontology*, 1976, Spec. Publ. 2.

Petrizzo, M.R., Falzoni, F., and Premoli Silva, I., Identification of the base of the Lower-to-Middle Campanian Globotruncana Ventricosa Zone: comments on reliability and global correlations, *Cretaceous Res.*, 2011, vol. 32, pp. 387–405.

Prakticheskoe rukovodstvo po mikrofaune. Radiolyarii mezozoya (Practical Manual on Microfauna. Cenozoic Foraminifers), St. Petersburg: Nedra, 1999 [in Russian].

Resheniya Vsesoyuznogo soveshchaniya po razrabotke unifitsirovannoi skhemy stratigrafii mezozoiskikh otlozhenii Russkoi platformy, sozvannogo 3-10 fevralya 1954 goda Geologicheskim upravleniem Ministerstva neftyanoi promyshlennosti SSSR (Resolutions of the All-Union Conference on Compilation of Unified Stratigraphic Charts for Mesozoic Deposits of the Russian Platform, February 3–10, 1954, Geological Survey Department, the USSR Ministry of Petroleum Industry), Leningrad: Gostopizdat, 1955 [in Russian].

Resheniya Vsesoyuznogo soveshcheniya po utochneniyu unifitsirovannoi skhemy stratigrafii mezozoiskikh otlozhenii Russkoi platformy (Resolutions of the All-Union Conference on Verification of Unified Stratigraphic Chart for Mesozoic Deposits of the Russian Platform), Leningrad: Gostoptekhizdat, 1962 [in Russian].

Robaszynski, F. and Christensen, W.K., The Upper Campanian–Lower Maastrichtian chalks of the Mons Basin, Belgium: a preliminary study of belemnites and foraminifera in the Harmignies and Ciply areas, *Geol. Mijnbouw*, 1989, vol. 68, pp. 391–408.

Schulz, M.-G., *Morphometrisch-variationsstatistische untersuchungen zur phylogenie der belemniten-gattung belemnella im Untermaastricht NW-Europas. (die Maastricht-Stufe in NW-Deutschland, Teil 1), Geol. Jbhrb.*, 1979, Part A, vol. 47.

Sel'tser, V.B. and Beniamovsky, V.N., Stages of evolution of chephalopods and benthic foraminifers as a basis of subdivision of the Campanian of East European Platform into three sub-stages, in *Mater. LX Sess. Paleontol. Obshch. pri RAN (7–14 aprelya 2014 g.)* (Proc. LX Paleontol. Soc. Russ. Akad. Sci. (April 7–14, 2014)), St. Petersburg: St. Petersburg, 2014, pp. 117–120.

Sinzow, I.F., Notizen über die Jura-, Kreide- und Neogen–Ablagerungen der Gouvernements Saratow, Simbirsk, Samara, und Orenburg, *Odessa Univ. Zap.*, 1899, vol. 77.

Stratigraficheskaya skhema verkhnemelovykh otlozhenii Vostochno-Evropeiskoi platformy (Stratigraphic Scheme of Upper Cretaceous Deposits in the East European Platform), St. Peterburg: Kart. Fabr. Vseross. Nauchno-Issled. Geol. Inst., 2004 [in Russian].

Stratigraficheskii kodeks Rossii (Stratigraphic Code of Russia), St. Peterburg: Vseross. Nauchno-Issled. Geol. Inst., 2006 [in Russian].

Stratigrafiya verkhn'ogo proterozoyu ta fanerozoyu Ukraïni u dvokh tomakh. T.1: Stratigrafiya verkhn'ogo proterozoyu, paleozoyu ta mezozoyu Ukraïni (The Upper Proterozoic and Phanerozoic Stratigraphy of Ukraine (in 2 vols). Vol. 1: Upper Proterozoic, Paleozoic, and Mesozoic Stratigraphy of Ukraine), Gozhik, P.F., Ed., Kyiv: IGN NAN Ukraïni. Logos, 2013. [in Ukrainian].

Streng, M., Hildebrand-Habel, T., and Willems, H., Long-term evolution of calcareous dinoflagellate associations since the Late Cretaceous: comparison of a high- and a low-latitude core from the Indian Ocean, *J. Nannoplankton Res.*, 2004, vol. 26, no. 1, pp. 13–45.

Subbotina, N.N., Foraminifers from Cretaceous and Paleogene deposits of the West Siberian Lowland, in *Tr. VNIGRI* (Proc. All-Russ. Petrol. Res. Explor. Inst.), 1964., vol. 234.

Thibault, N., Harlou, R., Schovsbo, N., et al., Upper Campanian–Maastrichtian nannofossil biostratigraphy and high-resolution carbon-isotope stratigraphy of the Danish Basin: towards a standard $\delta^{13}C$ curve for the Boreal Realm, *Cretaceous Res.*, 2012a, vol. 33, pp. 72–90.

Thibault, N., Husson, D., Harlou, R., et al., Astronomical calibration of Upper Campanian–Maastrichtian carbon isotope events and calcareous plankton biostratigraphy in the Indian Ocean (ODP Hole 762C): implication for the age of the Campanian–Maastrichtian boundary, *Palaeogeogr., Palaeoclimatol., Palaeoecol.*, 2012b, vols. 337–338, pp. 52–71.

Thibault, N., Anderskouv, K., Bjerager, M., et al., Upper Campanian–Maastrichtian chronostratigraphy of the Skælskør-1 core, Denmark: correlation at the basinal and global scale and implications for changes in sea-surface temperatures, *Lethaia*, 2015, vol. 48, no. 4, pp. 549–560.

Thibault, N., Harlou, R., Stemmerik, L., and Surlyk, F., Late Cretaceous (Late Campanian–Maastrichtian) sea-surface temperature record of the Boreal Chalk Sea, *Clim. Past*, 2016, vol. 12, pp. 429–438.

Umova, L.A., Tsatsur, G.I., and Shatrov, V.P., *Paleogeografiya vostochnogo sklona Urala i Zaural'ya v melovoe i paleotsenovoe vremya* (Cretaceous and Paleocene Paleogeography of the Eastern Slope of the Urals and the Trans-Urals), Sverdlovsk: Akad. Nauk SSSR, Ural. Fil., Inst. Geol. Geokhim., 1968 [in Russian].

Vishnevskaya, V.S., *Radiolyarievaya biostratigrafiya yury i mela Rossii* (Jurassic and Cretaceous Radiolarian Biostratigraphy of Russia), Moscow: GEOS, 2001 [in Russian].

Vishnevskaya, V.S., Radioplarian-based complexes and Cretaceous subdivisions of the Russian Plate, *Byull. RMSK po Tsentru i Yugu Russkoi Platformy*, Moscow: *RAEN*, 2009, vol. 4, pp. 67–84.

Vishnevskaya, V.S., Upper Cretaceous radiolarians of the East European Platform and their biostratigraphic significance, *Stratigr. Geol. Correl.*, 2010, vol. 18, no. 6, pp. 607–634.

Vishnevskaya, V.S., The first finding of calcareous dynocysts in the Maastrichtian deposits of the Volga River Region, in *Mater. God. sobr. (nauch. Konf.) sekt. Paleontol. MOIP i Mosk. Otd. Paleontol. obshch. pri RAN "Paleostrat-2015". Moskva, 26–28 yanvarya 2015 g.* (Annu. Meet. Paleontol. Group Moscow Soc. Nat. Explor. and Moscow Branch Paleontol. Soc. RAS "Paleostrat-2004"; Moscow, January 26–28, 2015), Alekseev, A.S., Ed., Moscow: Paleontol. Inst. RAN, 2015, pp. 23–24.

Vishnevskaya, V.S., Beniamovsky, V.N., Kopaevich, L.F., et al., New data on the Campanian-Maastrichtian boundary in the Volga River Region (foraminifers, radiolarians, nanoplankton, calcareous dynocysts), in *Sb. tr. XVI Vseross. mikropaleontol. soveshch. "Sovremennaya mikropaleontologiya"* (Proc. XVI All-Rus. Micropaleontol. Conf. "Modern Micropaleontology"), Tesakova, E.M., Ed., Kaliningrad, 2015, pp. 7–11.

Vishnevskaya, V.S., Ovechkina, M.N., Beniamovsky, V.N., Radiolarians from Santonian—Campanian reference sections of Saratov Povolzhie and correlation of subdivisions on calcareous nannoplankton, foraminifers, and radiolarians, *Bull. Mosk O-va Ispyt. Prir., Ser. Geol.*, 2014, vol. 89, no. 5, pp. 43–55.

Voigt, S., Friedrich, O., Norris, R.D., and Schönfeld, J., Campanian–Maastrichtian carbon isotope stratigraphy: shelf-ocean correlation between the European shelf sea and tropical Pacific Ocean, *Newslett. Stratigr.*, 2010, vol. 44, no. 1, pp. 57–72.

Voigt, S., Gale, A.S., Jung, C., and Jenkyns, H.C., Global correlation of Upper Campanian–Maastrichtian successions using carbon-isotope stratigraphy: development of a new Maastrichtian timescale, *Newslett. Stratigr.*, 2012, vol. 45, no. 1, pp. 25–53.

Van der Voo, R., *Palaeomagnetism of the Atlantic, Tethys, and Iapetus Oceans*, Cambridge: Cambridge Univ.Press, 1993.

Yakovishina, E.V., Korotaev, M.V., Kopaevich, L.F., et al., Substantiation of Upper Cretaceous stratigraphy of the Saratov Volga Region, in *Melovaya sistema Rossii i blizhnego zarubezh'ya: problemy stratigrafii i paleogeografii* (Cretaceous System of Russia and CIS Countries: Problems of Stratigraphy and Paleogeography), Krasnodar: Kuban. Gos. Univ., 2012, pp. 322–325.

Translated by I. Basov